

1-(Aryl)-6-[alkoxyalkyl]-3-azabicyclo[3.1.0]hexanes and 6-(Aryl)-6-[alkoxyalkyl]-3-azabicyclo[3.1.0]hexanes: A New Series of Potent and Selective Triple Reuptake Inhibitors

Fabrizio Micheli,^{*,†} Paolo Cavanni,[†] Roberto Arban,[†] Roberto Benedetti,[†] Barbara Bertani,[†] Michela Bettati,[†] Letizia Bettelini,[†] Giorgio Bonanomi,[†] Simone Braggio,[†] Anna Checchia,[†] Silvia Davalli,[‡] Romano Di Fabio,[†] Elettra Fazzolari,[†] Stefano Fontana,[†] Carla Marchioro,[‡] Doug Minick,^{‡,§} Michele Negri,[†] Beatrice Oliosi,[‡] Kevin D. Read,^{||} Ilaria Sartori,[†] Giovanna Tedesco,[‡] Luca Tarsi,[†] Silvia Terreni,[†] Filippo Visentini,[‡] Alessandro Zocchi,[†] and Laura Zonzini[†]

[†]Neurosciences Centre of Excellence for Drug Discovery, and [‡]Molecular Discovery Research, GlaxoSmithKline Medicine Research Centre, Via Fleming 4, 37135 Verona, Italy, [§]Molecular Discovery Research, GlaxoSmithKline, Five Moore Drive, Research Triangle Park, North Carolina, and ^{||}Biological Chemistry and Drug Discovery, College of Life Sciences, Sir James Black Centre, University of Dundee, Dundee DD1 5EH, Scotland, U.K.

Received December 9, 2009

The discovery of new highly potent and selective triple reuptake inhibitors is reported. The new classes of 1-(aryl)-6-[alkoxyalkyl]-3-azabicyclo[3.1.0]hexanes and 6-(aryl)-6-[alkoxyalkyl]-3-azabicyclo[3.1.0]hexanes are described together with detailed SAR. Appropriate decoration of the scaffolds was achieved with the help of a triple reuptake inhibitor pharmacophore model detailed here. Selected derivatives showed good oral bioavailability (> 30%) and brain penetration (B/B > 4) in rats associated with high in vitro potency and selectivity at SERT, NET, and DAT. Among these compounds, microdialysis and in vivo experiments confirm that derivative **15** has an appropriate developability profile to be considered for further progression.

Introduction

Drugs which are able to interfere with either the uptake or with the metabolism of aminergic neurotransmitters have been used for decades to treat depressed patients. The earliest medications, like monoamino oxidase (MAO) inhibitors or tricyclic antidepressants, gained a wide diffusion but are unfortunately linked to some side effects that may limit their efficacy.¹ More recently, drugs which act by selectively blocking neurotransmitter reuptake in either serotonergic neurons (SSRI, e.g., paroxetine, Figure 1) or noradrenergic neurons (SNRI, e.g., reboxetine, Figure 1) have become established as effective antidepressants. Furthermore, drugs which block reuptake at both serotonergic and noradrenergic transporters (e.g., venlafaxine, Figure 1) or at both noradrenergic and dopaminergic neurons (e.g., bupropion, Figure 1), also known as dual uptake inhibitors, provide good efficacy and tolerability too.¹

An important recent development has been achieved with the discovery of triple reuptake inhibitors² (TRUI) like indatraline, SEP-225289, or DOV derivatives, which are

reported in Figure 1. The idea behind a “broad-spectrum”^{2e} antidepressant that is capable of inhibiting amine uptake of the 5-HT,^a NE, and DA transporters comes from both preclinical^{2d–g} and clinical studies. It is known that dopamine agonists themselves (e.g., pergolide, bromocriptine) showed efficacy as augmenting agents with antidepressant in clinical studies.²ⁱ Accordingly, the contemporary block of the three aminergic neurotransmitters may produce, in addition to the elevation of 5-HT and NE, an increase in the CNS levels of DA. It has been hypothesized^{2b,e,h} that such specific increase in DA levels might address the anhedonic component of depression as well as shorten the time to onset. Therefore, the TRUI might result in improved efficacy toward a broader range of the depressed population.

Many of the TRUI templates reported to date show level of inhibition of the monoamine transporter such as SERT \cong NET \cong DAT.

In the quest for the identification of potent and selective TRUI, we report the discovery of a new series of 1-(aryl)-6-[alkoxyalkyl]-3-azabicyclo[3.1.0]hexanes, together with a new series of 6-(Aryl)-6-[alkoxyalkyl]-3-azabicyclo[3.1.0]hexanes, which are endowed with excellent pharmacokinetic (PK) properties in preclinical species and which work very effectively in different animal models related to the aminergic system.

During the past decade, part of GSK research focus in CNS drug discovery has aimed at the discovery of novel chemical entities able to influence the reuptake of aminergic neurotransmitters by their transporters and the rational design was followed to achieve this task and the development of two new potent and selective series based on azabicyclo[3.1.0]hexanes is reported here.

*To whom correspondence should be addressed. Phone: +39-045-8218515. Fax: +39-045-8118196. E-mail: Fabrizio.E.Micheli@gsk.com.

^aAbbreviations: hERG, human ether-a go-go K⁺ channel; NCE, novel chemical entity; PK, pharmacokinetic; P450, cytochrome P450; hCl_i, human intrinsic clearance; F%, bioavailability; B/B, brain/blood; Cl_b, blood clearance; V_d, distribution volume; SPA, scintillation proximity assay; 5-HT, serotonin; NE, norepinephrine or noradrenaline; DA, dopamine; SERT, serotonin transporter; NET, noradrenaline transporter; DAT, dopamine transporter; MD, microdialysis; pK_i, inhibition constant from binding assays; fpK_i, functional inhibition constant for an antagonist from functional assays e.g. functional inhibition constant obtained from inhibition functional assays using Cheng–Prusoff equation.

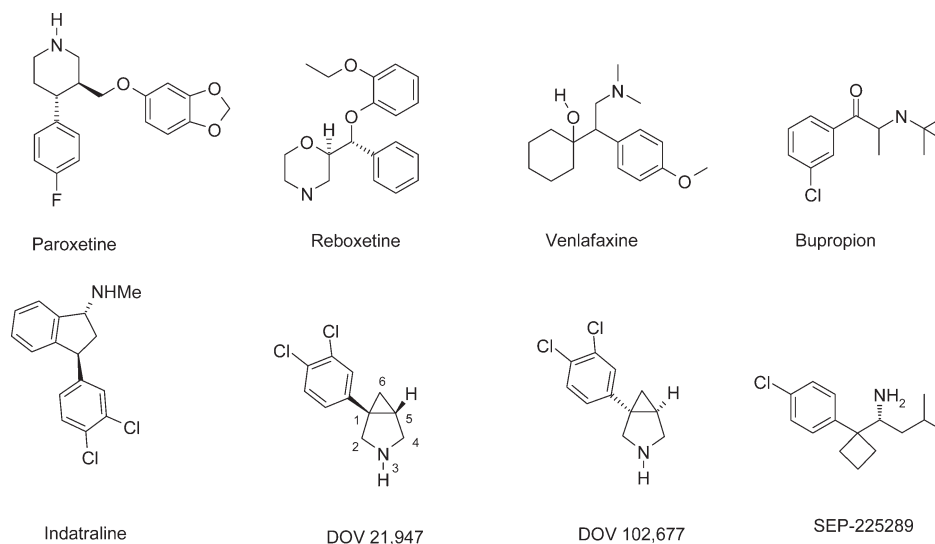


Figure 1. Structures of known monoaminergic reuptake inhibitors.

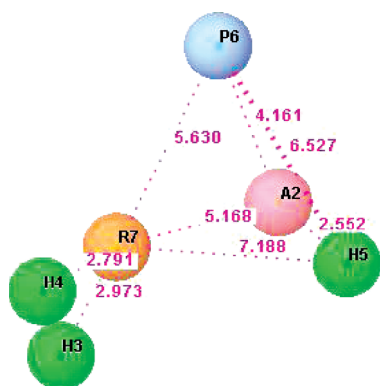


Figure 2. The triple reuptake inhibitors pharmacophore. Coding of features: blue sphere, positive ionizable; pink spheres, H-bond acceptor; green spheres, hydrophobic; orange sphere, aromatic ring. Distances among the pharmacophoric points are shown in angstroms.

Considering the in house expertise and the general information available in the literature, it was hypothesized that an appropriate decoration of the azabicyclo[3.1.0]hexane scaffold would have led to an increased affinity for the three aminergic transporters.

A TRUI pharmacophore model was developed in house exploiting both “mixed-activity” and selective transporter inhibitors, and more precisely, three specific pharmacophore models for SERT, NET, and DAT were built using structurally rigid and selective derivatives. These compounds derived both from GlaxoSmithKline’s proprietary collection and from the public domain (e.g., the examples reported in Figure 1 or in ref 3). The structures were modeled within the Maestro^{4a} modeling environment. Conformational analyses were carried out for the three structures with BatchMin^{4b} using the following parameters: 1000 steps/rotatable bond, OPLS_2005 FF, implicit water model of solvation, 5000 minimization steps with PRCG. Conformations lying within a 3 kcal/mol energy window were kept. A single-ligand pharmacophore was then built over these structures using the phase^{4c} module within Maestro and selecting the most relevant pharmacophoric features. The three pharmacophores were finally merged together to create the triple

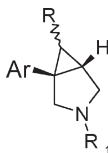
reuptake inhibitor pharmacophore. Average coordinates for the common pharmacophoric features were taken to determine their 3D arrangement, as illustrated pictorially in Figure 2. Further details can be found in the Supporting Information available.

Results and Discussion

Given the features exemplified in the pharmacophore model (Figure 2) and the relative distances among the pharmacophoric points there represented, it was decided to introduce an alkoxyalkyl side chain to potentially increase the point of interactions of the template with the transporter; in particular it was hypothesized that the ideal region to probe for a substituted azabicyclo[3.1.0]hexane was represented by the position 6 of the same scaffold, having been the position 5 previously explored in house in the past without any substantial improvement in the potency of the scaffold. It is also important to notice that, in this specific pharmacophore model, some uncertainty is related to the role of the H-bond acceptor mapped by the ether motif. An ether oxygen in general is not a particularly strong H-bond acceptor, and it may well be that this pharmacophoric point is an artifact, as this atom is present in topologically equivalent positions in all the compounds used to derive the pharmacophore.

The compounds belonging to this new series were prepared in agreement to the synthetic route reported in Scheme 1 and results are reported in Table 1. In particular, in our quest for the “ideal” triple reuptake inhibitor the desired profile was defined as a compound having relative affinities in the order $SERT \geq NET > DAT$, thus allowing the study in vivo of an alternative profile to the currently existing derivatives where $SERT \cong NET \cong DAT$. A different in vitro profile may theoretically account for a different in vivo read-out either in terms of desired activity or potential side effects.

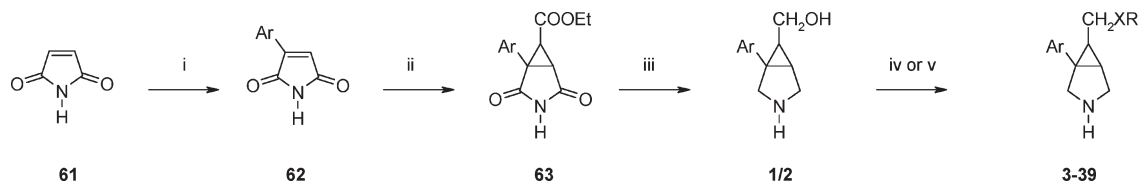
All the compounds prepared were assayed for their capacity to bind to the three monoamine transporters (SERT, NET, and DAT) in SPA-binding primary assays on membranes from cells transiently transduced with BacMam virus. Additionally, the ability of the most interesting compounds to block [³H]5-HT, [³H]NE, and [³H]DA uptake were evaluated in functional uptake SPA assays using LLCPK cells stably

Table 1. Binding at the Three Transporters (SERT, NET, DAT) Expressed as pK_i^a 

entry	stereochemistry	R	R ₁	Ar	hSERT SPA pK _i	hNET SPA pK _i	hDAT SPA pK _i
DOV 21,947	NA	NA	H	NA	7.70	7.20	6.90
DOV 102,677	NA	NA	H	NA	6.70	6.10	6.70
1	endo (rac)	CH ₂ OH	H	3,4-di Cl Ph	7.29	6.74	6.32
2	exo (rac)	CH ₂ OH	H	3,4-di Cl Ph	7.81	7.54	6.34
3	exo (rac)	CH ₂ OMe	H	3,4-di Cl Ph	8.82	8.50	6.96
4	endo (rac)	CH ₂ OMe	H	3,4-di Cl Ph	7.14	5.89	6.18
5	exo (se)	CH ₂ OMe	H	3,4-di Cl Ph	9.12	8.76	7.25
6	exo (se)	CH ₂ OMe	H	3,4-di Cl Ph	7.59	6.65	6.29
7	exo (rac)	CH ₂ OCH ₂ c-Pr	H	3,4-di Cl Ph	9.02	8.71	7.60
8	exo (se)	CH ₂ OCH ₂ c-Pr	H	3,4-di Cl Ph	8.30	7.80	6.70
9	exo (se)	CH ₂ OCH ₂ c-Pr	H	3,4-di Cl Ph	9.50	9.20	7.90
10	endo (rac)	CH ₂ OCH ₂ c-Pr	H	3,4-di Cl Ph	7.50	6.90	6.30
11	exo (rac)	CH ₂ On-Pr	H	3,4-di Cl Ph	9.30	9.30	7.70
12	exo (se)	CH ₂ On-Pr	H	3,4-di Cl Ph	8.02	7.50	6.60
13	exo (se)	CH ₂ On-Pr	H	3,4-di Cl Ph	9.60	9.20	7.90
14	exo (rac.)	CH ₂ OEt	H	3,4-di Cl Ph	9.40	8.80	7.60
15	exo (se)	CH ₂ OEt	H	3,4-di Cl Ph	9.80	9.30	8.10
16	exo (se)	CH ₂ OEt	H	3,4-di Cl Ph	7.60	6.70	6.70
17	exo (se)	CH ₂ OEt	Me	3,4-di Cl Ph	8.90	7.80	7.40
18	exo (rac)	CH ₂ OCH ₂ CF ₃	H	3,4-di Cl Ph	8.90	8.40	7.30
19	exo (se)	CH ₂ OCH ₂ CF ₃	H	3,4-di Cl Ph	7.25	6.46	6.20
20	exo (se)	CH ₂ OCH ₂ CF ₃	H	3,4-di Cl Ph	9.20	8.80	7.60
21	exo (rac)	CH ₂ O <i>i</i> -Pr	H	3,4-di Cl Ph	9.70	9.40	8.10
22	exo (se)	CH ₂ O <i>i</i> -Pr	H	3,4-di Cl Ph	7.40	6.70	6.60
23	exo (se)	CH ₂ O <i>i</i> -Pr	H	3,4-di Cl Ph	9.90	9.60	8.30
24	exo (rac)	CH ₂ O <i>c</i> -butyl	H	3,4-di Cl Ph	9.20	8.90	7.90
25	exo (se)	CH ₂ O <i>c</i> -butyl	H	3,4-di Cl Ph	9.50	9.30	8.40
26	exo (se)	CH ₂ O <i>c</i> -butyl	H	3,4-di Cl Ph	7.60	6.80	6.60
27	exo (rac)	CH ₂ O <i>c</i> -pentyl	H	3,4-di Cl Ph	9.30	9.10	8.20
28	exo (se)	CH ₂ O <i>c</i> -pentyl	H	3,4-di Cl Ph	9.60	9.80	8.60
29	exo (se)	CH ₂ O <i>c</i> -pentyl	H	3,4-di Cl Ph	8.10	7.90	7.00
30	exo (rac)	CH ₂ O <i>c</i> -hexyl	H	3,4-di Cl Ph	9.00	8.70	7.70
31	exo (rac)	CH ₂ O(4-F-phenyl)	H	3,4-di Cl Ph	8.90	7.40	7.10
32	exo (rac)	CH ₂ NMe ₂	H	3,4-di Cl Ph	8.40	7.50	6.20
33	exo (rac)	CH ₂ SMe	H	3,4-di Cl Ph	9.10	8.30	7.10
34	exo (se)	CH ₂ SMe	H	3,4-di Cl Ph	9.40	8.80	7.40
35	exo (se)	CH ₂ SMe	H	3,4-di Cl Ph	7.60	6.50	7.20
36	exo (rac)	<i>n</i> -Pr	H	3,4-di Cl Ph	9.00	8.70	7.60
37	exo (rac)	CH ₂ OMe	H	2-naphthyl	9.80	9.00	7.30
38	exo (se)	CH ₂ OMe	H	2-naphthyl	7.90	6.50	6.40
39	exo (se)	CH ₂ OMe	H	2-naphthyl	10.10	9.20	7.60

^aSEM for hSERT/NET/DAT data sets is ± 0.1 . (rac) = racemate. (se) = single enantiomer. NA = Not applicable.

Scheme 1. General Synthetic Procedures for the Preparation of Compounds 1–39^a



^aX = O, S, C; Ar = naphthyl for derivatives 37, 38, 39, and 3,4-dichlorophenyl for the other mentioned compounds. (i) ArNH₂, CuCl₂, tBuNO₂, CH₃CN, 0 °C; (ii) Me₂SCH₂CO₂Et⁺ Br⁻, NaH, or ethyldiazoacetate/THF 0 °C to rt; (iii) BH₃-THF in THF at reflux; (iv) (a) BOC₂O, TEA, CH₂Cl₂, (b) NaH, RX in THF/DMF, (c) TFA, CH₂Cl₂ 0 °C to rt; (v) (a) BOC₂O, CH₂Cl₂, (b) MsCl/Et₃N followed by R₁ONa or R₂ONa or RMgBr, (c) TFA, CH₂Cl₂ 0 °C to rt.

transfected with human SERT, NET, or DAT. These more interesting compounds also underwent filtration binding as-

says on membranes prepared from LLCPK cells stably transfected with each of the three human transporters.

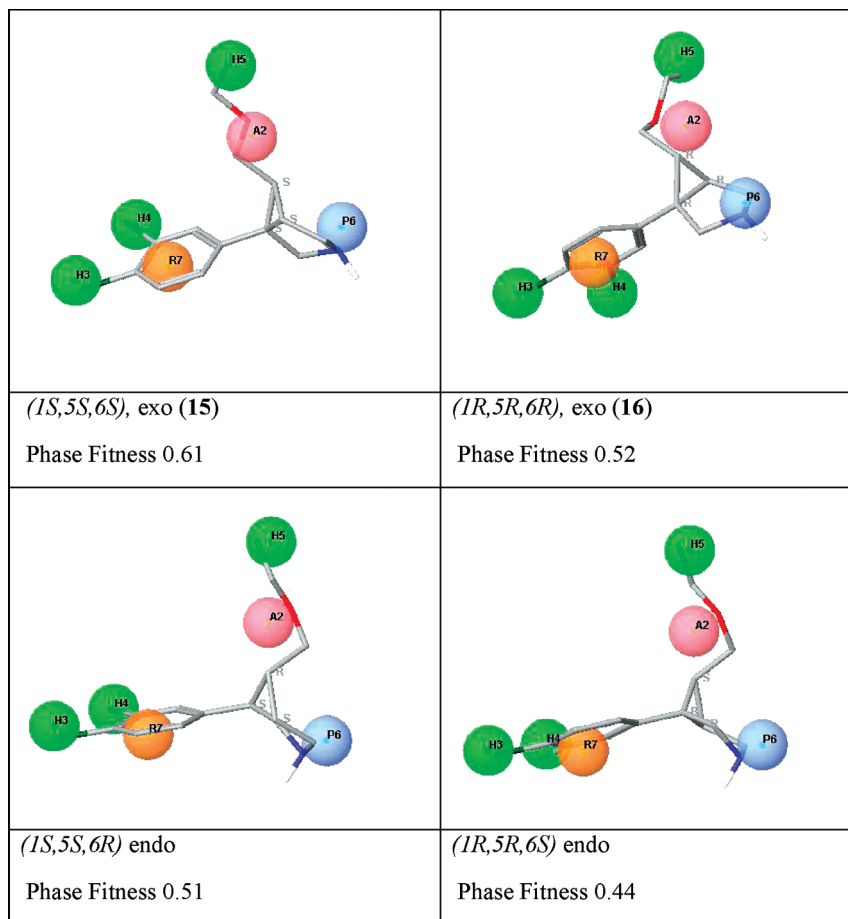
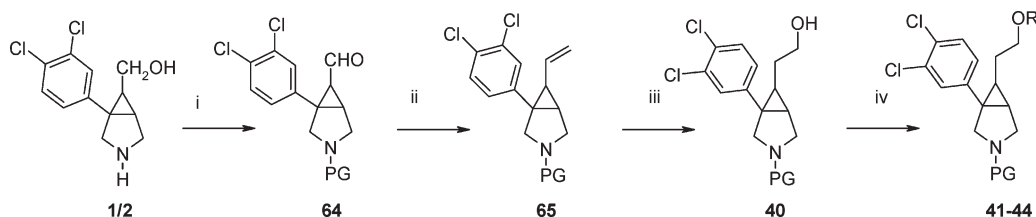


Figure 3. The exo derivatives **15** and **16** fitted in the pharmacophore model in comparison with the potential endo isomers. It can be clearly seen, both in terms of visual overlapping and in terms of phase Fitness (ranging from 0 to 1, the higher the better), that the triple reuptake inhibitors pharmacophore superimposes much better with the exo isomers with respect to the corresponding endo isomers.

Furthermore, to ensure that the selected templates were endowed with appropriate developability characteristics from the beginning of the exploration, the NCEs went through generic developability screens such as CYPEX bactosome P450 inhibition and rat and human in vitro clearance in liver microsomes early in the screening cascade.

Given the route described in Scheme 1, the first compound to be tested was the intermediate alcohol prepared with the 3,4-dichlorophenyl aryl derivative so to directly compare with literature standard derivatives. This compound was separated into its endo (**1**) and exo (**2**) derivatives, and both compounds were tested as racemate. Interestingly enough, the introduction of the hydroxymethyl group had no major effect on the affinity for the transporters with respect to the unsubstituted derivative; nonetheless, a significant difference was observed between the endo and exo compound toward both SERT and NET affinity, while no major difference was noticed over DAT activity. The following alkylation of the alcohol to the corresponding methyl ether further increased this gap, with the exo derivative **3** much more active than the corresponding endo one (**4**); furthermore, in agreement with the original design, the introduction of this group greatly increased both SERT and NET affinity and also led to a moderate DAT affinity increase. The separation of the racemate **3** by chiral chromatography led to the single enantiomers **5** and **6**. Derivative **5** showed a nanomolar affinity at SERT and similar affinity over NET, while the DAT affinity was about 70-fold lower. The compound was also tested using filtration

assay binding conditions, and the values obtained were in good agreement with the SPA binding ($pK_i = 9.13/8.34/7.07$ on SERT/NET/DAT respectively); finally, the rat-SERT native tissue binding in filtration was also verified, leading to a $pK_i = 8.75$. To verify, since the beginning, if the introduction of the alkoxyalkyl side chain was appropriate in terms of developability of the potential new class, **5** was further assayed in agreement to the above-described screening cascade. IC_{50} values for all major P450 isoforms tested (CYP1A2, CYP2C9, CYP2C19, CYP2D6, and CYP3A4) were greater than $6 \mu\text{M}$ and intrinsic clearance (Cl_i) values both in human and in rat resulted moderately low (<0.5 and 3.8 mL/min/g of protein). Considering this positive in vitro data, the pharmacokinetic (PK) profile in vivo in rat was evaluated;⁵ derivative **5** showed a relatively low blood clearance ($Cl_b = 16 \text{ mL/min/kg}$), leading to an appropriate half-life for in vivo testing in appropriate disease models ($t_{1/2} = 2.4 \text{ h}$). The distribution volume was also relatively low ($V_d = 2.9 \text{ L/kg}$) and the bioavailability was excellent ($F = 94\%$). Considering that central nervous system (CNS) is the final target for this class of molecules, brain penetration was evaluated too. The compound demonstrated a brain/blood (B/B) ratio of 4, with a brain fraction unbound of 2.7% showing excellent penetration properties and low tissue binding values. Very encouraged by these initial results, which could be considered as the discovery of an interesting dual SERT/NET derivative, the investigation on this class was further expanded. The major objectives of the exploration

Scheme 2. General Synthetic Procedures for the Preparation of Compounds **40–44**^a

^a PG = H or BOC (i) (a) BOC₂O, TEA, CH₂Cl₂, (b) Dess–Martin periodinane; (ii) Me(Ph)₃P⁺Br⁻, BuLi, THF; (iii) (a) BH₃–THF, THF, (b) NaOH, H₂O₂ 30%, (c) TFA, CH₂Cl₂ 0 °C to rt; (iv) NaH, RX in THF/DMF; (c) TFA, CH₂Cl₂ 0 °C to rt.

were related to the dimension of the pocket available for binding within the transporter, to its sensitivity to polarity, and to the role played by the oxygen bridge. The introduction of a bulky cyclopropyl methyl derivative (**7–9**) was well tolerated, leading to a very potent molecule (**9**) on each of the three transporters; in particular, the greater relative increase was obtained on the dopamine transporter. The bulkiness was well tolerated also in terms of developability properties with all of the P450 isoforms inhibited with IC₅₀ greater than 10 μM with the exception of CYP2C19 and CYP2D6 (IC₅₀ = 3 and 1 μM, respectively). Human and rat Cl_i were comparable to derivative **5** despite a higher lipophilicity of the molecule (<0.5 and 2.6 mL/min/g of protein, respectively). The in vivo PK evaluation in rat of derivative **9** demonstrated that the good results achieved by **5** were not related to a singleton derivative; actually, the compound, despite a higher lipophilicity, was still endowed with acceptable PK parameters: Cl_b was high (72 mL/min/kg) with a high volume of distribution (5.2 L/kg), leading to a reduced half-life (*t*_{1/2} = 1 h). Bioavailability was moderate (*F* = 32%) and the brain penetration very high (B/B = 10), although this was driven by higher nonspecific binding as the key parameter, fraction unbound, was very low (*F*_{ub} = 0.1%). As observed for the previous compounds, also in this case the endo derivative was much less potent (**10**). Therefore, considering the superiority of the exo substitution with respect to the endo one, the exploration was continued on the former template. This experimental result was also in agreement with the predictions of the pharmacophore model used during the planning of the series. Actually, when all the four potential stereoisomers of the [3.1.0] scaffold were fitted in the model, the exo derivatives showed a better fit than the corresponding endo ones as exemplified in Figure 3.

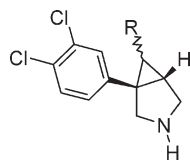
The introduction of a linear and slightly less lipophilic moiety (*n*-Pr, **11–13**) led to a superimposable in vitro profile of derivative **13** with **9**, both from the primary binding at the transporters and from the DMPK point of view. The further reduction by one carbon atom (Et, **14–16**) led to similar affinity properties (**15**) but greatly improved in vitro DMPK characteristics. All of the major P450 isoforms were inhibited with IC₅₀ greater than 9 μM with one exception (CYP2D6 IC₅₀ = 4 μM) and human and rat Cl_i were relatively low (1.2 and 1.3 mL/min/g of protein, respectively). The in vivo PK profile in rat was excellent too: **15** showed low Cl_b (18 mL/min/kg) and distribution volume (*V*_d = 1.4 L/kg), with acceptable half-life (*t*_{1/2} = 1.2 h) and very good bioavailability (*F* = 61%). Brain penetration was good (B/B = 4.6) as well as the fraction unbound (1.4%).

Considering its overall profile, **15** was further characterized and shown to efficiently inhibit the uptake of all of the three monoamines (pIC₅₀ = 8.90/9.80/8.30 on SERT/NET and DAT, respectively). However, whereas the functional pIC₅₀

observed in the DAT assay was in line with the affinity of **15** in the respective binding assay, the functional pIC₅₀ observed at NET was higher than the binding affinity for NET. On the contrary, functional potency of **15** at SERT was lower than its binding affinity for this transporter. With the latter, it is important to notice that a difference was expected because the SERT uptake-SPA assay is known to be particularly sensitive to test conditions (e.g., cell numbers) and, from previous in house experience, most SERT blockers tested in uptake assays showed pIC₅₀ values lower than the corresponding affinity in the binding assay. However, because pIC₅₀ values are a relative measure of compounds potency, being dependent on assay conditions, reliable comparison of the functional potency of the compounds at the three monoamine transporters is not possible. Therefore, the results of these functional uptake studies are to be considered only indicative of the likely functional ratio of effect in vivo, whereas the binding affinities must be considered a reliable basis on which to predict a potential in vivo effect.

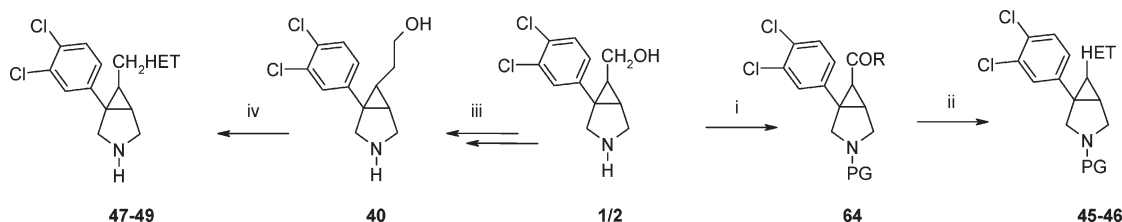
N-Methylation of the secondary amine, **17**, led to approximately a 10-fold decrease in affinity at the three transporters, while the introduction of a dipole in the system (**18–20**) gave a 5-fold decrease (**20**). Moreover, the replacement of the terminal methyl group with a CF₃ derivative, despite a higher lipophilicity, did not substantially change the in vitro DMPK parameters and gave a similar in vivo PK profile (Cl_b = 42 mL/min/kg; *V*_d = 3.2 L/kg; *t*_{1/2} = 1.4 h; *F* = 41%); the major differences were observed in terms of brain penetration and fraction unbound (B/B = 18; *F*_{ub} = 0.6%). The introduction of a branching alpha to the oxygen atom (*i*-Pr, **21–23**) further increased the affinity for the three transporters (**23** vs **13**) by about 2.5-fold and was not detrimental for the in vitro developability profile (IC₅₀ greater than 8 μM on all major P450 isoforms; human and rat Cl_i = 1.4 and <0.5 mL/min/kg, respectively). A further increase in bulkiness had no major impact on affinity (*c*-butyl, **24–26**; *c*-pentyl **27–29**) with slightly higher NET values for **28** and started to become detrimental with the introduction of the bulkiest *c*-hexyl derivative **30**, still maintaining high levels of affinity on all the three transporters. The introduction of an aromatic moiety, **31**, had no major impact on SERT affinity but led to a more marked decrease in terms of NET and DAT when compared to **30**.

Compared to the parent racemic compound **4**, the introduction of a strong polar component (NMe₂, **32**) had no major impact in terms of loss of affinity; actually, the NET affinity decreased 10-fold while the SERT and DAT affinity decreased approximately 5-fold. The original question relating to the real existence of an H-bond acceptor feature in the pharmacophore model was potentially answered in the following steps. The replacement of the oxygen with a sulfur atom (**32–34**) potentially demonstrates that the ether probably

Table 2. Binding at the Three Transporters (SERT, NET, DAT) Expressed as pK_i^a 

entry	stereochemistry	R	hSERT SPA pK_i	hNET SPA pK_i	hDAT SPA pK_i
40	exo (rac)	CH ₂ CH ₂ OH	8.60	8.10	7.10
41	exo (rac)	CH ₂ CH ₂ OMe	9.10	8.50	7.20
42	exo (se)	CH ₂ CH ₂ OMe	9.60	9.00	7.30
43	exo (se)	CH ₂ CH ₂ OMe	7.50	6.00	6.90
44	exo (rac)	CH ₂ CH ₂ OEt	9.10	8.40	7.10
45	exo (rac)	5-methyl-1,3-oxazol-2-yl	7.80	7.70	6.90
46	exo (rac)	4-methyl-1,3-thiazol-2-yl	9.00	8.00	7.50
47	exo (rac)	CH ₂ (4-methyl-1,3-thiazol-2-yl)	9.70	9.50	7.70
48	exo (se)	CH ₂ (4-methyl-1,3-thiazol-2-yl)	10.10	9.90	7.70
49	exo (se)	CH ₂ (4-methyl-1,3-thiazol-2-yl)	7.80	7.10	7.30

^aSEM for hSERT/NET/DAT data sets is ± 0.1 . (rac) = racemate. (se) = single enantiomer.

Scheme 3. General Synthetic Procedures for the Preparation of Compounds **45–49**^a

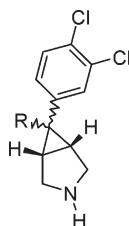
^aPG = H or BOC, R = OH or NHalk, HET = heterocycle (i) (a) Jones reagent at 0 °C in CH₂Cl₂, (b) HOBT, EDC, NH₄R; (ii) (a) heating with appropriate halo-ketone, (b) TFA, CH₂Cl₂ 0 °C to rt; (iii) steps from (i) to (iii) in Scheme 2; (iv) (a) Jones reagent at 0 °C in CH₂Cl₂, (b) HOBT, EDC, NH₄OH, (c) Lawesson's reagent, (d) heating with appropriate halo-ketone, (e) TFA, CH₂Cl₂ 0 °C to rt.

does not constitute a weak hydrogen-bond acceptor in the transporter. The slightly higher lipophilicity of **34** compared to **5** has a slight impact on SERT but leaves NET and DAT affinity almost unaltered within experimental error. This evidence is also potentially confirmed by the replacement of the oxygen with a carbon atom where the racemate **36** is not different from the corresponding racemate **14** as far as NET and DAT are concerned and show a 2-fold decrease in terms of SERT affinity. Finally, among the different aryl derivative tested in the exploration (data not shown), in this specific series of derivatives, the 2-naphthyl group (**37–39**) seems to act well as 3,4-dichlorophenyl bioisoster. Actually, in this specific series, **39** showed a 10-fold higher SERT affinity with respect to **5** and approximately a 5-fold affinity increase over NET and DAT, leading to a picomolar affinity compound on serotonin transporter. In this case, human and rat Cl_i were 2.2 and 3.9 mL/min/kg, respectively, and the CYP450 inhibition profile showed IC₅₀ greater than 4 μM for all the major P450 isoforms except CYP1A2 (0.9 μM).

In the second part of the exploration, the ether position was moved one position further down the apical side chain and the compounds were prepared in agreement with the general Scheme 2, and the results are reported in Table 2. Also in this case, the first compound to be tested as racemate was the exo intermediate alcohol **40**. Compared to the corresponding racemic derivative **2**, this compound showed an average increase of 5-fold in terms of affinity on the three transporters. Methylation of the alcohol led to derivatives **41–43**; the increased chain length of **42** compared to derivative **5** led to

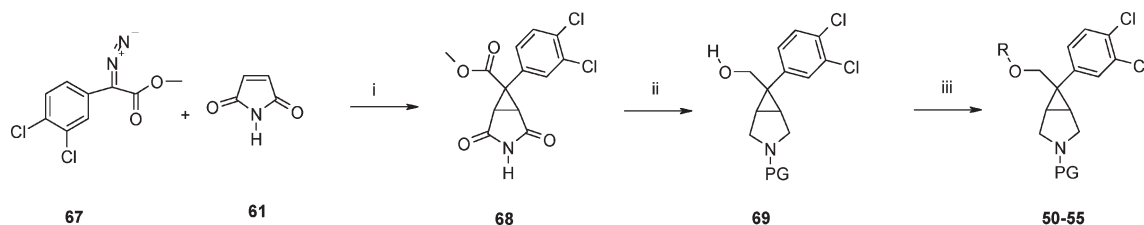
a 5-fold increase in the SERT activity, and a 2–3-fold increased affinity in terms of NET and DAT. The compound was tested for its ability to inhibit the uptake of the monoamines giving a pIC₅₀ of 8.80/9.40/7.80 on SERT, NET, and DAT respectively. Once again, the lower activity observed on SERT compared to the binding results has to be considered in light of the explanation previously reported. The increase in length of the ether chain from methyl to ethyl group (from **41** to **44**) did not show the same increase observed moving from **3** to **14**, possibly suggesting that the side chain had already reached the best fitting or explored the maximum length tolerated by the binding pocket. To probe if this was the case, some specific heterocycles were prepared according to the synthetic Scheme 3 and the results are reported in Table 2.

The oxazolyl derivative **45** was probably able to pick up no more interactions than derivative **2**, but its introduction was not detrimental for activity, confirming the availability of enough space in that region of the transporter; the slightly more lipophilic thiazolyl derivative **46** actually acted in the expected direction, increasing the affinity on the transporters by about 5-fold, confirming the general trend achieved up to that point of the exploration. Interestingly enough, the elongation of such a molecule (**47–49**) led to the very potent derivative **48**; differently from the 2-naphthyl derivative **39**, in this case not only the SERT affinity was picomolar but also the NET affinity was in the low nanomolar range with the DAT comparable and about 100-fold lower, thus leading to the identification of another potential dual activity derivative. For confirmation, experiments of reuptake were performed

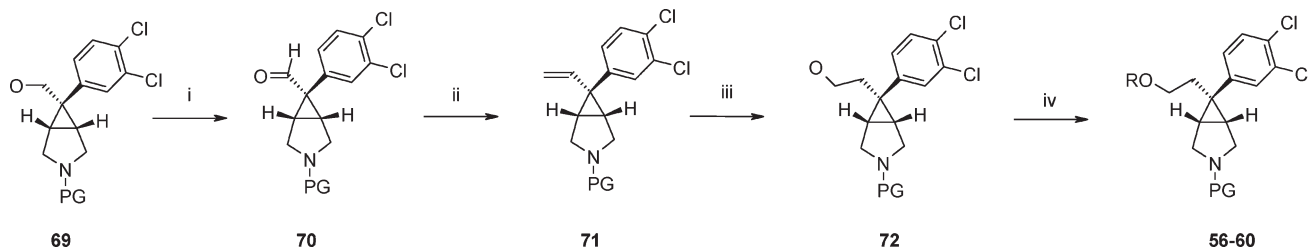
Table 3. Binding at the Three Transporters (SERT, NET, DAT) Expressed as pK_i^a 

entry	stereochemistry	R	hSERT SPA pK_i	hNET SPA pK_i	hDAT SPA pK_i
50	exo	CH ₂ OEt	9.30	7.90	7.70
51	endo	CH ₂ OEt	5.60	4.60	5.20
52	exo	CH ₂ OCH ₂ <i>c</i> -Pr	9.20	8.10	8.00
53	exo	CH ₂ O <i>c</i> -butyl	9.40	8.60	8.20
54	exo	CH ₂ OCH ₂ CF ₃	9.00	7.60	7.60
55	exo (rac)	CH ₂ O <i>sec</i> -butyl	9.60	8.70	8.10
56	exo	CH ₂ CH ₂ OMe	9.50	8.10	8.00
57	exo	CH ₂ CH ₂ OEt	9.30	8.10	7.80
58	exo	CH ₂ CH ₂ O <i>i</i> Pr	9.50	8.80	8.20
59	exo (rac)	CH ₂ CH ₂ O <i>sec</i> -butyl	9.50	8.40	8.30
60	exo	CH ₂ CH ₂ O <i>c</i> -butyl	9.70	8.40	8.20

^a SEM for hSERT/NET/DAT data sets is ± 0.1 . (rac) = racemate, referred to the nature of the *sec*-butyl alcohol used.

Scheme 4. General Synthetic Procedures for the Preparation of Compounds **50–55**^a

^a PG = H or BOC; (i) toluene, reflux; (ii) BH₃-THF, refluxing THF; (iii) (a) RX, NaH, DMF from 0 °C to rt, (b) TFA, CH₂Cl₂ 0 °C to rt.

Scheme 5. General Synthetic Procedures for the Preparation of Compounds **56–60**^a

^a PG = H or BOC; (i) (a) BOC₂O, TEA, CH₂Cl₂, (b) Dess–Martin periodinane; (ii) Me(Ph)₃P⁺Br⁻, BuLi, THF; (iii) (a) BH₃-THF, THF, (b) NaOH, H₂O₂ 30%; (iv) (a) or MsCl/TEA in CH₂Cl₂ 0 °C to rt followed by R₂ONa in DMF, (b) TFA, CH₂Cl₂ 0 °C to rt.

and **48** gave pIC_{50} of 9.00/9.60/7.70 on SERT, NET, and DAT, respectively.

To complete the exploration, given the new information provided for the pharmacophore model, it was decided to keep the side chain in position 6 of the bicyclic template and to move also the 3,4-dichlorophenyl derivative in the same position as a potential positive overlap might also have arisen from this combination. The results of the exploration are reported in Table 3, and the compounds were prepared according to Scheme 4 for the alkoxy methylene substituent and following Scheme 5 for the alkoxyethylene derivatives. On this new scaffold, the presence of a plane of symmetry leads to a pro-chiral situation in which the aryl ring can sit exo or endo. In Table 2 the definition (rac) for racemate is referred

only to the nature of the *sec*-butyl alcohol used in the coupling. By comparing derivatives **50** and **51**, it is possible to infer that the extended exo derivatives appear to provide a better fitting within the three transporters binding site, leading to a compound with high affinity for all of them. Once again, this was in agreement with the pharmacophore model predictions as reported in Figure 4. Derivative **50** also showed a positive P450 profile with IC₅₀ values greater than 5 μ M on all the isoforms. Unfortunately, it was not as metabolically stable, with Cl_i values slightly higher than in the previous template (h- and r-Cl_i being 3.4 and 5.1 mL/min/g of protein, respectively). The introduction of the cyclopropyl methyl substituent (**52**) led to a slight DAT affinity increase, while a bulkier alpha branched cyclo-butyl moiety (**53**) led to a substantial increase

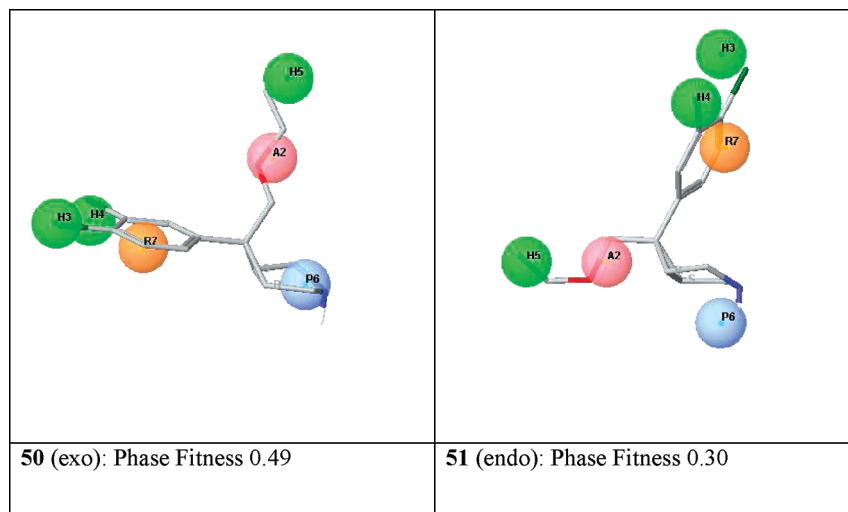


Figure 4. The exo derivative **50** fitted in the pharmacophore model in comparison with the endo isomer **51**.

of both NET and DAT components, resulting in a very balanced triple reuptake inhibitor. These modifications led to a slight change in the P450 profile of the derivatives, with **52** having IC_{50} values greater than $10\ \mu M$ on all the isoforms with the exception of CYP2D6 and CYP3A4 DEF ($IC_{50} = 1$ and $4\ \mu M$, respectively) and **53** having IC_{50} values greater than $10\ \mu M$ on all the isoforms with the exception of CYP3A4 DEF ($IC_{50} = 3\ \mu M$). The introduction of a slight dipole (**54**, $-CH_2CF_3$) with respect to **50** had no major effect on the affinity at the three transporters but introduced a potential liability in the P450 profile with the IC_{50} of direct inhibition of CYP2D6 = $0.3\ \mu M$. The presence of an α branching (*s*-Butyl, **55**) endowed with higher conformational freedom when compared to **53** did not alter neither the primary affinity profile nor the positive P450 profile. The introduction of a further methylene to extend the position of the ether in the space is represented by derivatives **56–60**. For derivatives **56** and **57**, no major effect on the primary affinity profile was observed, but unfortunately **57** showed a potential liability in the P450 profile (CYP2D6, $IC_{50} < 0.1\ \mu M$). The introduction of the α branching (**58–60**) had a positive effect on the affinity, in particular on DAT being **60**, another potent and selective triple reuptake inhibitor, with no major effect on the previously observed P450 profile.

Among the potent dual and triple reuptake inhibitors identified in the exploration, it was decided to select some of the best derivatives to be further characterized along the screening cascade, and derivative **15** is here reported as a model.

Further Characterization of Derivative 15. The first step for a more complete characterization of **15** was the determination of its absolute stereochemistry. The stereochemistry of this molecule and its enantiomer **16** were assigned using vibrational circular dichroism (VCD),⁶ and derivative **15** was identified as the (1*S*,5*S*,6*S*) isomer in accordance to the methodology reported in the Experimental Section. Interestingly enough, as reported in Figure 3, the pharmacophore model was also able to correctly identify the chirality of best fitting isomer **15**.

The second step of the characterization, in agreement with the screening cascade, was related to increasing the information on the selectivity of the compound using a panel of binding and functional assays available in house. The

compound showed at least 100-fold selectivity over a wide range of receptors, with the most notable results here reported (adrenergic α_{1A} , $fpK_i = 6.7$; 5-HT_{2A}, $fpK_i = 6.8$; H1, $fpK_i = 6.0$; muscarinic acetylcholine receptor: M1, $fpK_i = 6.8$; M2, $fpK_i = 6.7$; M3, $fpK_i = 7.2$; M4, $fpK_i = 6.6$; M5, $fpK_i = 7.0$). The compound was also submitted to a hERG electrophysiology assay⁷ to assess its overall activity for this K^+ channel, and the results ($IC_{50} 4.2\ \mu M$) confirmed the hERG binding affinity ($pK_i = 4.9$).

Considering the possibility to test **15** in vivo in preclinical species, the compound was tested in rat native tissues (filtration binding) where it showed an excellent profile with $pK_i = 9.17/9.87/7.87$ on SERT, NET, and DAT, respectively. The higher affinity on rat NET was also observed for other compounds of the same series and was also common to some standard derivatives. This is in line with a generally increased affinity for rat NET observed for other compounds in comparison to the human transporter and might support the existence of a species difference in NET pharmacology. Mouse SERT filtration binding data were also generated, and the compound showed a $pK_i = 9.07$, in good agreement with the above-reported rat data.

Considering its overall balanced profile in terms of primary activity and PK properties, and considering the desired ratio among the human transporters with SERT \geq NET $>$ DAT (ratio $\approx 1/3/50$), it was decided to explore the in vivo behavior of the compound. Nonetheless, considering that the rat profile showed a NET \geq SERT $>$ DAT, a further preliminary step was considered necessary to fully interpret the final results. Because of its mode of action, **15** was expected to increase the extracellular concentration of monoamines as measured by in vivo microdialysis.

To test this hypothesis, microdialysis probes were implanted in the medial prefrontal cortex (MPC) in freely moving rats with concurrent locomotor activity measurement and quantification of NE, DA, and 5-HT brain levels⁸ by HPLC analysis and electrochemical detection. Derivative **15** was tested at 0.1, 0.3, and 1 mg/kg (ip) and, as reported in Figure 5, at the highest dose tested, it induced a slow and sustained increase in the levels of the monoamines that lasted throughout the experiment (3 h post treatment); this was particularly significant for DA levels. At the same time, an increased locomotor activity was observed in rat at the same

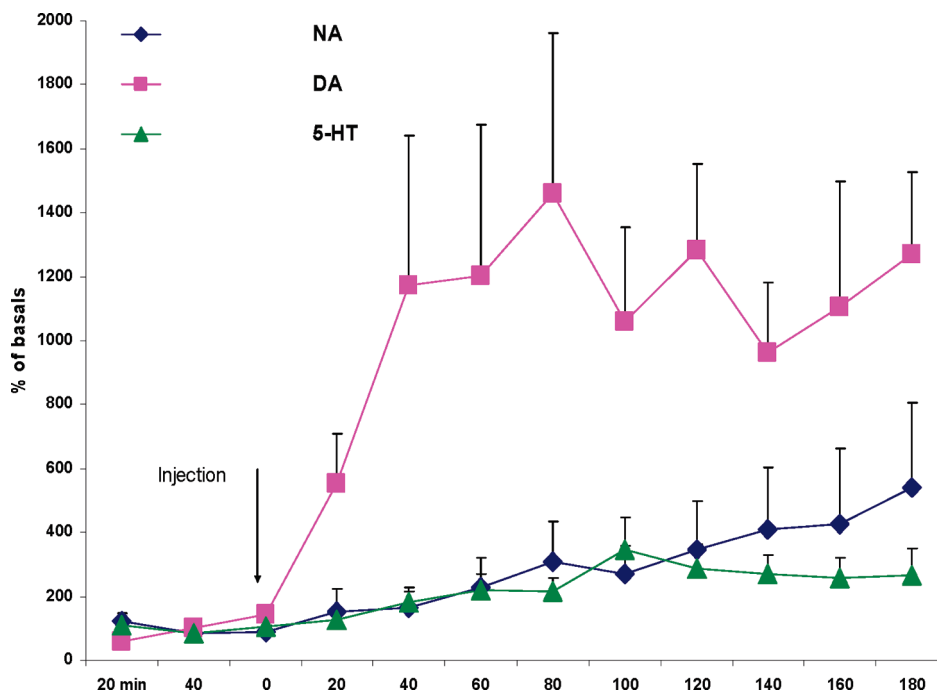


Figure 5. Time course of the effect of **15** on norepinephrine (diamond), dopamine (square), and serotonin (triangle) outflow in the rat medial prefrontal cortex. Arrow shows injection. Data are mean \pm SEM of neurotransmitter concentration expressed as percentage of basal values. Doses tested = 1 mg/kg, ip.

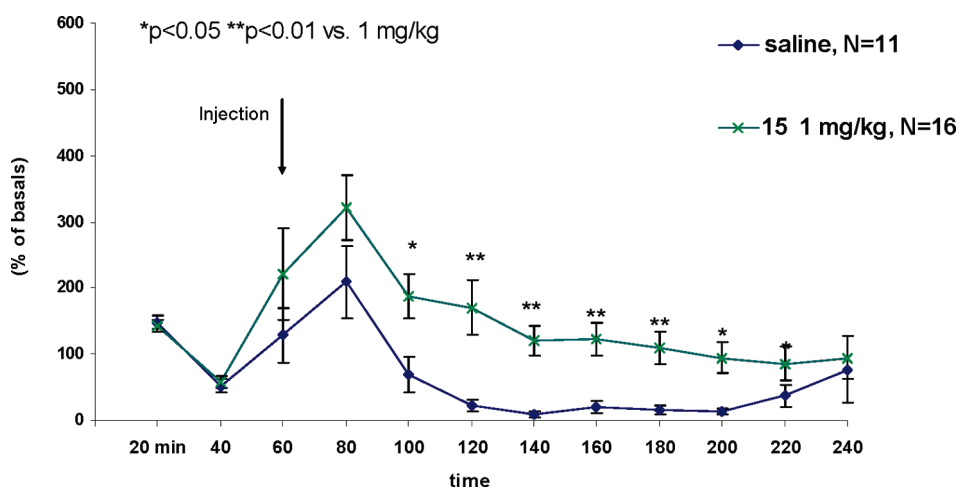


Figure 6. Time course of the effect of **15** on rat locomotor activity at 1 mg/kg ip.

dose (Figure 6). These results demonstrate that the acute administration of **15** produced a slow onset/long lasting increase in the extracellular levels of all monoamines in MPC in rats, in agreement with the triple reuptake inhibitor profile.

At this point, **15** was tested in three in vivo models in mice to further confirm its ability to inhibit the monoamine transport and produce antidepressant-like effects.

In the first of these experiments (Figure 7, right), it was tested in the 5-hydroxytryptophan (5-HTP) potentiation assay.⁹ The compound was administered orally 2 h before the experiment. The results demonstrate that **15** significantly increased in a dose dependent manner 5-HTP stereotyped behavior at 3, 10, and 30 mg/kg. In the same study, the standard SSRI drug citalopram significantly increased 5-HTP stereotyped behavior. Accordingly, these data confirm in vivo the inhibition of the 5-HT transporter.

In the second experiment (Figure 7, center), **15** was evaluated for its effects on spontaneous locomotor activity in the rat.¹⁰ The compound was administered orally 2 h before the experiment at 3, 10, and 30 mg/kg and it was found to significantly increase locomotor activity at 10 mg/kg., while the lack of effect at 30 mg/kg was unforeseen. The data are consistent with an increased dopaminergic neurotransmission due to the inhibition of the DA transporter by **15**.

In the last experiment, the potential antidepressant-like effect of **15** was evaluated in the forced swimming test¹¹ (FST), which is sensitive to known antidepressant drugs (Figure 7, left). Once again, the compound was administered orally 2 h before the test in mice at 1, 3, and 10 mg/kg. As clearly seen in the figure, **15** significantly reduced immobility time at 3 and 10 mg/kg as predicted by its in vitro and PK profile. However, the possibility that the increase in

15 was administered p.o. 120 min before tests

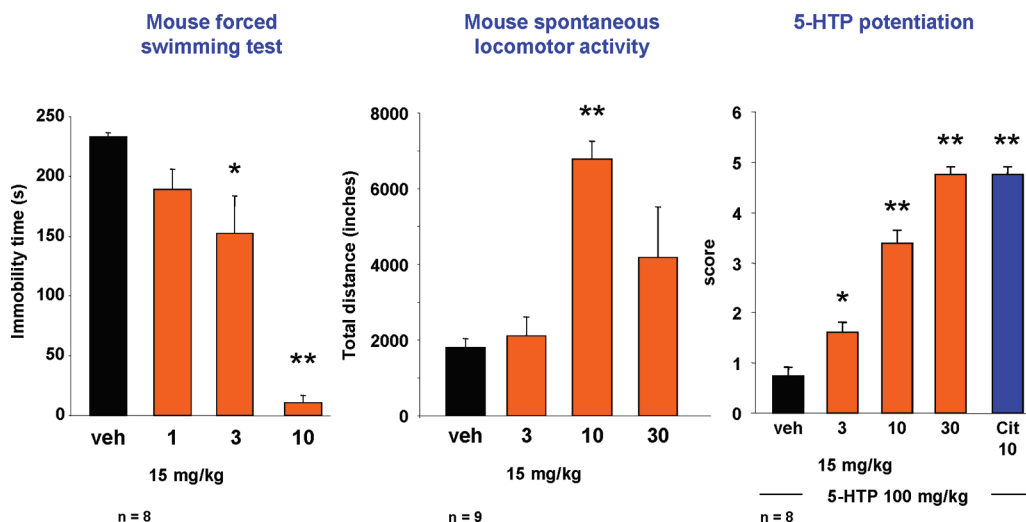


Figure 7. Effects of derivative **15** in the FST model (left panel) on the spontaneous locomotor activity (middle panel) and in the 5-HTP model (right panel) in mice.

locomotor activity (in rats) in the same dose range could have affected the results of the FST cannot be ruled out.

Conclusions

The planned introduction of an appropriate side chain into a 1-(aryl)-3-azabicyclo[3.1.0]hexane template and its transformation into a 6-(aryl)-6-[alkoxyalkyl]-3-azabicyclo[3.1.0]hexane scaffold led to the identification of two different classes of potent and selective triple reuptake inhibitors. These molecules are endowed with an excellent developability profile and showed activity in preclinical animal models related to the increase of the monoamines.

Derivative **15**, in particular, was used to probe the role of a system in which SERT, NET, and DAT are appropriately chosen in a given ratio. MD and in vivo experiments performed on this molecule clearly indicate its mode of action through monoamine uptake inhibition.

Experimental Section

Biological Test Methods. In Vitro Studies. Filtration Binding Assay for Human Recombinant SERT, NET, and DAT. Filtration binding assays were run using membranes prepared from LLCPC cells stably transfected with each of the three human transporters. Filtration [³H]citalopram binding assay for human SERT (hSERT) was conducted in deep-well 96-well plate in a total volume of 404 μ L/well by adding 4 μ L of test compound (100 \times solution in neat DMSO) or DMSO (to define total binding) or a final concentration of 10 μ M fluoxetine (to define nonspecific binding, NSB), 200 μ L of 0.25 nM [*N*-methyl-³H]citalopram (Amersham Biosciences, 80 Ci/mmol) and 200 μ L of hSERT-LLCPC membranes (about 2.5 μ g protein/well). After 2 h at room temperature, the reaction was stopped by rapid filtration through GF/B Unifilter 96-filter plate (Perkin-Elmer) presoaked in 0.5% polyethylenimine (PEI) using a Perkin-Elmer FilterMat-196 harvester. Filterplate was washed 3 times with 1 mL/well ice-cold 0.9% NaCl solution, dried, and finally 50 μ L of Microscint 20 (Perkin-Elmer) were added to each well. The radioactivity was counted using Top-Count liquid scintillation counter (Packard-Perkin-Elmer) and recorded as counts per minute (CPM). Data analysis was performed by using a 4-parameter logistic equation with GraphPad PRISM software and p*K*_i has been calculated from pIC₅₀ by

using the Cheng–Prusoff equation. Competition binding assay for human NET (hNET) was conducted essentially as previously reported for SERT except for the use of hNET-LLCPC cell membranes (4.8 μ g/well), 1.5 nM of [*N*-methyl-³H]nisoxetine as radioligand (Amersham Biosciences, 84 Ci/mmol), and 10 μ M desipramine for NSB. Finally, the same procedure was adopted also for human DAT (hDAT) competition binding assay but using hDAT/LLCPC cell membranes (9.6 μ g/well), 10 nM [*N*-methyl-³H]WIN-35,428 (Perkin-Elmer, 85.6 Ci/mmol), and 10 μ M GBR-12909 for NSB.

Filtration Binding for Rat Native SERT, NET, and DAT and Mouse Native SERT. Filtration binding studies were carried out on rat and mouse brain native tissue. The affinity of the compound was determined on rat or mouse cortex for SERT, on rat hippocampus for NET, and on rat striatum for DAT by using the appropriate radioligand. Competition binding assays for rat and mouse SERT, rat NET, and rat DAT were conducted essentially as previously reported for human recombinant monoamine transporters but using a different amount of membranes (20 and 7 μ g of protein /well for rat and mouse SERT binding, 40 and 20 μ g/well for rat NET and DAT binding, respectively).

hERG-[³H] Dofetilide Binding Assay. hERG activity was measured using ³H dofetilide binding in a scintillation proximity assay (SPA) format. The activity was measured with a PerkinElmer Viewlux imager.

SPA-Binding for Human Recombinant SERT, NET, and DAT. The affinity of the compounds to the human transporters has been assessed with radioligand displacement binding of [³H]citalopram, [³H]nisoxetine, and [³H]WIN-35,428 for SERT, NET, and DAT in BacMam-recombinant human SERT, NET, and DAT membranes with the SPA technology. Briefly, 0.3 μ L of test compound were added by 30 μ L of the SPA mixture, containing 1 mg/mL SPA (GE HealthCare, RPNQ0260) beads (SERT) or 2 mg/mL SPA beads (NET and DAT), 6 or 40 or 20 μ g/mL of SERT or NET or DAT BacMam membranes, 0.02% Pluronic F-127, 3 nM [³H]citalopram, or 10 nM [³H]nisoxetine or 10 nM [³H]WIN-35,428 for SERT or NET or DAT binding SPA in the assay buffer (20 mM HEPES, 145 mM NaCl, 5 mM KCl, pH 7.4). Incubation was performed overnight at room temperature. Bound radioactivity was measured with the Viewlux instrument. Data analysis was performed by using a four-parameter logistic equation with ActivityBase software and p*K*_i has been calculated from pIC₅₀ by using the Cheng–Prusoff equation.

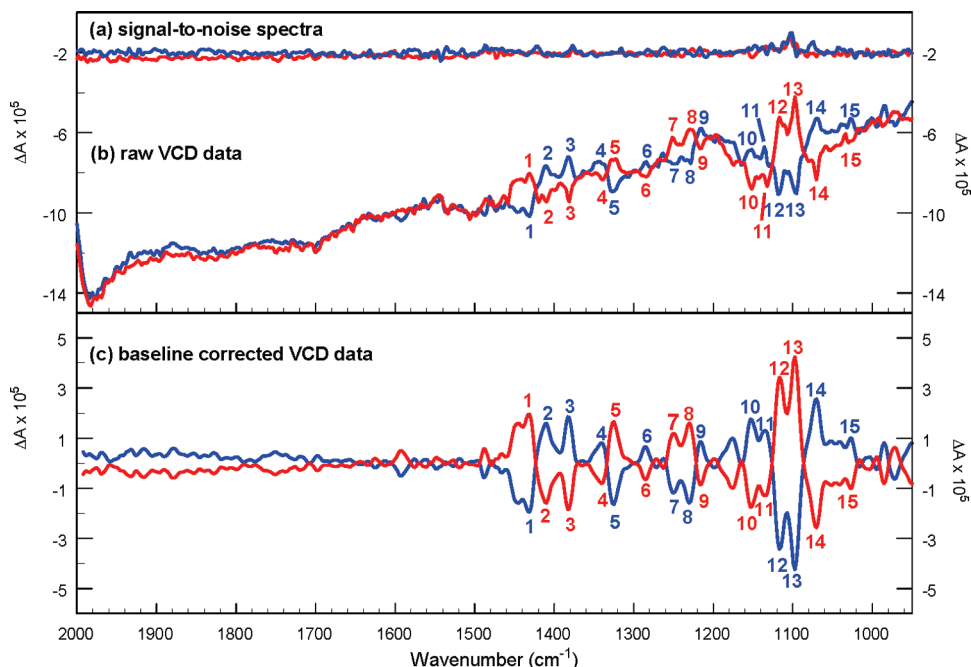


Figure 8. Upper panel: signal-to-noise and raw VCD spectra of **15** (red) and **16** (blue). Lower panel: baseline corrected VCD spectra of **15** (red) and **16** (blue). Bands in the experimental assignment set have been labeled in raw and baseline corrected VCD data.

Functional Uptake for SERT, NET, and DAT. The potency of the compounds in blocking the [^3H]serotonin, [^3H]noradrenalin, and [^3H]dopamine uptake was evaluated in a functional uptake-SPA assay on LLCPK cells stably transfected with human SERT, NET, and DAT. Briefly, 0.2 μL of test compound were added by 10 μL of the bead-cell SPA mixture, containing 1.5 mg/mL SPA beads (SERT and NET) or 2 mg/mL of SPA beads (DAT), 25000 or 50000 or 75000 cell/well of SERT or NET or DAT LLCPK cells, 0.02% Pluronic F-127 in the assay buffer (20 mM HEPES, 145 mM NaCl, 5 mM KCl, pH 7.4). The uptake was started by the substrate addition of 10 μL of 35 nM [^3H]serotonin or 45 nM [^3H]noradrenalin or 75 nM [^3H]dopamine for SERT or NET or DAT uptake SPA. Incubation was performed at room temperature for 1 h. Uptake was measured with the Viewlux instrument and data analysis was performed as before.

P450 CYP450 Assay. Inhibition (IC_{50}) of human CYP1A2, 2C9, 2C19, 2D6, and 3A4 was determined using Cypex Bactosomes expressing the major human P450s. A range of concentrations (0.1, 0.2, 0.4, 1, 2, 4, and 10 μM) of test compound were prepared in methanol and preincubated at 37 $^{\circ}\text{C}$ for 10 min in 50 mM potassium phosphate buffer (pH 7.4) containing recombinant human CYP450 microsomal protein (0.1 mg/mL; Cypex Limited, Dundee, UK) and probe-fluorescent substrate. The final concentration of solvent was between 3 and 4.5% of the final volume. Following preincubation, NADPH regenerating system (7.8 mg glucose 6-phosphate, 1.7 mg NADP and 6 units glucose 6-phosphate dehydrogenase/mL of 2% (w/v) NaHCO_3 ; 25 μL) was added to each well to start the reaction. Production of fluorescent metabolite was then measured over a 10 min time-course using a Spectrafluor plus plate reader. The rate of metabolite production (AFU/min) was determined at each concentration of compound and converted to a percentage of the mean control rate using Magellan (Tecan software). The inhibition (IC_{50}) of each compound was determined from the slope of the plot using Grafit v5 (Erithacus software, UK). Miconazole was added as a positive control to each plate. CYP450 isoform substrates used were ethoxyresorufin (ER; 1A2, 0.5 μM), 7-methoxy-4-trifluoromethylcoumarin-3-acetic acid (FCA; 2C9, 50 μM), 3-butyryl-7-methoxycoumarin (BMC; 2C19, 10 μM), 4-methylaminomethyl-7-methoxycoumarin

(MMC; 2D6, 10 μM), diethoxyfluorescein (DEF; 3A4, 1 μM) and 7-benzyloxyquinoline (7-BQ; 3A4, 25 μM). The test was performed in three replicates.

Intrinsic Clearance (CL_i) Assay. Intrinsic clearance (CL_i) values were determined in rat and human liver microsomes. Test compounds (0.5 μM) were incubated at 37 $^{\circ}\text{C}$ for 30 min in 50 mM potassium phosphate buffer (pH 7.4) containing 0.5 mg microsomal protein/mL. The reaction was started by addition of cofactor (NADPH; 8 mg/mL). The final concentration of solvent was 1% of the final volume. At 0, 3, 6, 9, 15, and 30 min an aliquot (50 μL) was taken, quenched with acetonitrile containing an appropriate internal standard, and analyzed by HPLC-MS/MS. The intrinsic clearance (CL_i) was determined from the first-order elimination constant by nonlinear regression using Grafit v5 (Erithacus Software, UK), corrected for the volume of the incubation and assuming 52.5 mg microsomal protein/g of protein for all species. Values for CL_i were expressed as mL/min/g of protein. The lower limit of quantification of clearance was determined to be when <15% of the compound had been metabolized by 30 min and this corresponded to a CL_i value of 0.5 mL/min/g of protein. The upper limit was 50 mL/min/g of protein.

VCD. Experimental VCD and IR spectra were acquired in the 2000–800 cm^{-1} frequency range using a BioTools ChiralIR FT-VCD spectrometer operating at 4 cm^{-1} resolution. Samples were analyzed in CDCl_3 at approximate concentrations of 10 mg/125 μL . Harmonic frequencies and corresponding vibrational intensities were calculated using Gaussian 98 ((Gaussian '98, Gaussian, Inc., Pittsburgh, PA (www.gaussian.com/index.htm)). Predicted gas-phase harmonic frequencies were shifted to the condensed phase region using a uniform scaling factor of 0.98.

The observed and baseline-corrected VCD data for **15** and **16** are shown in Figure 8. The signs of the 15 marker bands identified in these spectra were used to assign the configurations. The VCD and IR spectra observed for **15** are compared in Figure 9a with VCD and IR spectra calculated for a full structure model with (1*S*,5*S*,6*S*) configuration. In the upper panel of this figure, marker bands in the observed VCD spectrum have the same signs as corresponding marker bands in the calculated VCD spectrum, indicating that this

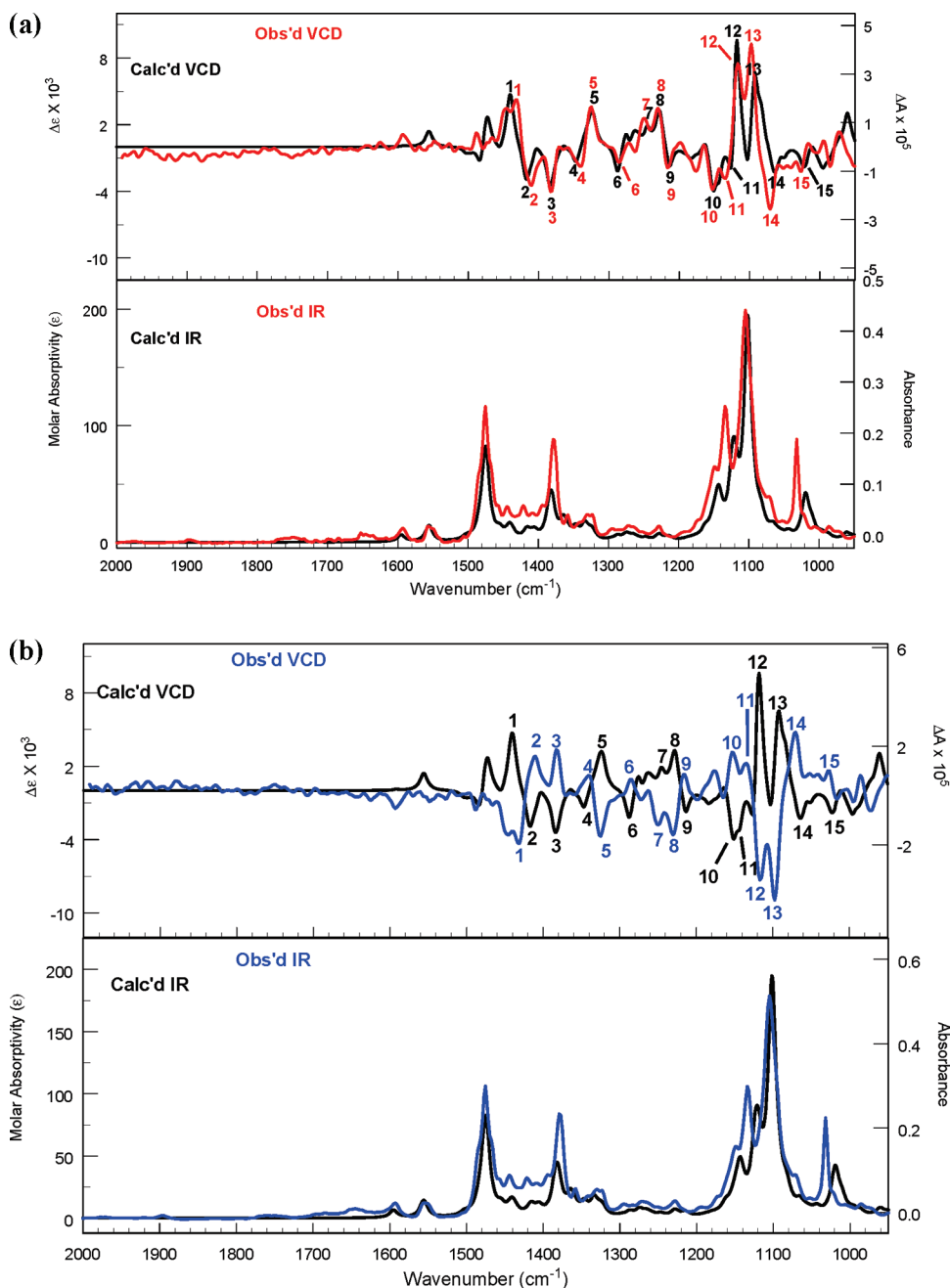


Figure 9. (a) Upper panel: VCD spectrum of **15** (red) vs calculated VCD spectrum (black). Lower panel: IR spectrum of **15** (red) compared with calculated IR spectrum (black). Bands in the experimental assignment set have been labeled in both experimental and calculated VCD spectra. (b) Upper panel: VCD spectrum of **16** (blue) vs calculated VCD spectrum (black). Lower panel: IR spectrum of **16** (blue) compared with calculated IR spectrum (black). Bands in the experimental assignment set have been labeled in both experimental and calculated VCD spectra.

enantiomer has the same absolute configuration as the model. Therefore, **15** was assigned as the (1*S*,5*S*,6*S*)-isomer. The VCD and IR spectra observed for **16** are compared in Figure 9b with the same calculated and VCD and IR spectra. In this case, marker bands in the experimental VCD spectrum are oppositely signed relative to the corresponding marker bands in the calculated VCD spectrum, indicating that **16** is the mirror image enantiomer of the model, and therefore was assigned as the (1*R*,5*R*,6*R*)-isomer. Close overall agreement between calculated and observed VCD and IR spectra in Figures 9a and 9b indicates that these assignments are highly reliable.

In Vivo Studies. All experiments were prereviewed and approved by a local animal care committee in accordance with the

guidelines of the “Principles of Laboratory Animal Care” (NIH publication no. 86–23, revised 1985), and with a project license that was obtained according to Italian law (Art. 7, Legislative Decree no. 116, 27 January 1992), which acknowledges European Directive 86/609/EEC on the care and welfare of laboratory animals.

Naive male CD-1 mice (Charles River, Italy) weighing 25–30 g were used in the 5-HTP potentiation test, in the forced swimming test, and for the assessment of spontaneous locomotor activity.

5-HTP Potentiation. The administration of the precursor of 5-hydroxytryptophan (5-HTP) to mice leads to a serotonergic syndrome characterized by stereotypic behavior. The combination monoamine reuptake inhibitors with subthreshold doses of

5-HTP has been proposed as a model to evaluate in vivo effects of drug acting at the serotonin transporter (Ortmann, 1980).

Mice were pretreated with **15** 120 min before an intraperitoneal (ip) injection of 5-HTP (100 mg/kg) and placed individually into a perspex box (20.5 cm × 20.5 cm × 34 cm). Experiments were videotaped and the following behaviors were scored for the following 30 min: aimless hyper locomotor activity (aHLMA), abduction of hind limbs (HLA), flat body posture (FBP), head twitches/tremor (HT), body tremor (BT). Each behavior was scored either present (scored = 1) or absent (scored = 0) by an observer blind to the drug treatment.

Forced Swimming Test. The mouse forced swimming test (Porsolt et al., 1977) is widely used as an animal model for detecting and screening antidepressant activity. Mice were dropped individually into glass cylinders (height 25 cm, diameter 10 cm) containing 10 cm water maintained at $25 \pm 1^\circ\text{C}$ and left there for 6 min. A mouse was judged immobile when it floated in an upright position and made only small movements to keep its head above water. The duration of immobility was recorded during the last 4 min of the 6 min testing period. All experiments were videotaped, and an observer who was unaware of the drug treatment scored immobility.

Compound **15** was administered orally 120 min before test.

Spontaneous Locomotor Activity. Spontaneous locomotor activity was measured by using activity boxes equipped with infrared monitoring sensors (AccuScan model RXYZXCM-16, Columbus, OH). Each box (40 cm × 40 cm × 30.5 cm) was made of clear plexiglas and covered with a plexiglas lid with air-holes with infrared sensors located along the perimeter 2.5 cm above the floor. Data were collected and analyzed (AccuScan model CDA-8, Columbus, OH). Animals were treated orally with compound **15** 120 min before test, and spontaneous locomotor activity quantified as total distance traveled, was recorded over 30 min.

MD and Locomotor Activity Data. Animals. Male CD rats (Charles River, Italy), weighing between 280 and 310 g at the beginning of the experiment, were housed in constant conditions of temperature ($21 \pm 1^\circ\text{C}$) and moisture, under a 12 h light/dark cycle with water and food available ad libitum. They were handled every day to get accustomed to manipulation and presence of researchers.

Intracerebral Microdialysis Surgery. Animals were anesthetized with proper concentrations of medetomidine hydrochloride (Domitor) and Xylazine (Zoletil) while Carprofren (Rymadil) was injected to induce analgesia. They were then placed on a stereotaxic apparatus for small animals. A guide cannula was lowered and positioned above the left medial prefrontal cortex (anteroposterior 3.2 mm; lateral 0.5 mm; dorsoventral 1.8 mm from bregma) or nucleus accumbens (anterior: +1.7 mm; ventral: -6.0 mm; mediolateral: 1.2 mm from bregma) and secured to the skull using dental cement, anchored by four stainless steel screws. A removable stainless steel stylet was placed inside the cannula to maintain its patency throughout the experimental period. Following surgery, the animals were injected with atipamezole hydrochloride (antisedan), and rubrocillin antibiotic and housed in single cages for one week to recover.

Microdialysis Experiment. The day before the experiment the stylet was removed from the guide cannula and a microdialysis probe with a 4-mm-long membrane was inserted (MAB 4 Agnho's, Sweden). The following day microdialysis experiments were performed in their home cage. Both inlet and outlet of the probe were attached with FEP tubings (dead volume 1.2 $\mu\text{L}/10\text{ cm}$) to a dual quartz lined two-channel liquid swivel (model 375/D/22QM Instech Laboratories, Plymouth Meeting PA) mounted on a low mass spring counterbalanced arm (MCLA, Instech). One channel was connected to a gastight syringe (Hamilton 1002 LTN 2.5 mL, Bonaduz, Switzerland) on a microinfusion pump (the Univentor 802 syringe pump) to deliver artificial cerebrospinal fluid (KCl 2.5 mM, NaCl 125

mM, CaCl_2 1.3 mM, MgCl_2 1.18 mM, Na_2HPO_4 2 mM, pH 7.4 with H_3PO_4 85%) at a steady flow rate of 1.1 $\mu\text{L}/\text{min}$, and the second channel was connected to a refrigerated fraction collector (Univentor 820 Microsampler) containing microtubes with 3 μL of 1 mM oxalic acid solution. Length of the outlet tubing was calculated to achieve a 20 min delay of sample collection. Samples were collected every 20 min and frozen in dry ice for subsequent HPLC analysis. Two hours of perfusion were allowed before starting the experiment.

Probe Localization. The position of the probe in the brain areas was verified at the end of each experiment. A blue dye was injected through a probe without the dialysis membrane and the brains were then removed and coronally sectioned at the level of the PFC or NAc. Trace localization was visually identified through comparison with a stereotaxic atlas of rat brain (Paxinos and Watson, 2005). Animals with incorrect probe position were discarded from the final analysis.

HPLC Procedure. NA, DA, and 5-HT concentrations were determined in dialysate samples by HPLC with electrochemical detection (Antec Decade). Separation was achieved using a mobile phase consisting of 12 mM Na_2HPO_4 , 88 mM NaH_2PO_4 , 5 mM NaCl, 0.1 mM EDTA· Na_2 , 20% MeOH, 10% MeCN, pH 6.00 ± 0.05 . Chromatographic data were acquired and processed through Empower software.

Data Analysis. For each animal absolute neurochemical data in pg were transformed in % values vs average of the three basal values. They were preliminary analyzed with 2D Box and Whiskers plot to determine and eliminate outlier and extreme values. Data eliminated were substituted with the mean of the same group at the same time. Final data were analyzed with two-way ANOVA for repeated measures with treatment and time as factors. Whenever allowed, preplanned post hoc multiple comparisons were applied to compare time points of different treatments.

Concurrent general motor activity was measured through an automated digital video analysis of animal movements (ViewPoint). Data were analyzed as previously described for microdialysis data.

Chemical Procedures. General. Experimental Section. Proton magnetic resonance (NMR) spectra are typically recorded either on Varian instruments at 300, 400, or 500 MHz or on a Bruker instrument at 300 and 400 MHz. Chemical shifts are expressed in δ (ppm) units, and peak multiplicity are expressed as follows: singlet (s), doublet (d), doublet of doublets (dd), triplet (t), multiplet (m), broad singlet (br s), broad multiplet (br m). The NMR spectra were recorded at a temperature ranging from 25 to 90°C . When more than one conformer was detected, the chemical shifts for the most abundant one was reported.

Mass spectra (MS) are typically taken on a 4 II triple quadrupole mass spectrometer (Micromass UK) or on a Agilent MSD 1100 mass spectrometer, operating in ES (+) and ES (-) ionization mode or on an Agilent LC/MSD 1100 mass spectrometer, operating in ES (+) and ES (-) ionization mode coupled with HPLC instrument Agilent 1100 series [LC/MS-ES (+): analysis performed on a Supelcosil ABZ +Plus (33 mm × 4.6 mm, 3 μm) (mobile phase: 100% [water + 0.1% HCO_2H] for 1 min, then from 100% [water + 0.1% HCO_2H] to 5% [water + 0.1% HCO_2H] and 95% [CH_3CN] in 5 min, finally under these conditions for 2 min; $T = 40^\circ\text{C}$; flux = 1 mL/min; LC/MS-ES (-): analysis performed on a Supelcosil ABZ +Plus (33 mm × 4.6 mm, 3 μm) (mobile phase: 100% [water + 0.05% NH_3] for 1 min, then from 100% [water + 0.05% NH_3] to 5% [water + 0.05% NH_3] and 95% [CH_3CN] in 5 min, finally under these conditions for 2 min; $T = 40^\circ\text{C}$; flux = 1 mL/min]; in the mass spectra, only one peak in the molecular ion cluster is reported.

DAD chromatographic traces, mass chromatograms, and mass spectra may be taken on a on a UPLC/MS Acquity system coupled with a Micromass ZQ mass spectrometer operating in ESI positive or negative. The phases used are: (A) $\text{H}_2\text{O}/\text{ACN}$ 95/5 + 0.1% TFA; (B) $\text{H}_2\text{O}/\text{ACN}$ 5/95 + 0.1% TFA. The gradient

is: $t = 0$ min, 95%A 5%B; $t = 0.25$, 95%A 5%B; $t = 3.30$, 100%B, $t = 4.0$) 100%B, followed by 1 min of reconditioning.

Flash silica gel chromatography was carried out on silica gel 230–400 mesh (supplied by Merck AG Darmstadt, Germany) or over Varian Mega Be–Si prepacked cartridges or over prepacked Biotage silica cartridges. SPE-SCX cartridges are ion exchange solid phase extraction columns supplied by Varian. The eluent used with SPE-SCX cartridges is methanol followed by 2N ammonia solution in methanol. In a number of preparations, purification was performed using either Biotage manual flash chromatography (Flash+) or automatic flash chromatography (Horizon, SP1) systems. All these instruments work with Biotage Silica cartridges. SPE-Si cartridges are silica solid phase extraction columns supplied by Varian.

The enantiomeric purity of each single enantiomer obtained after preparative chromatography on chiral columns was always verified on analytical column.

The purity of the compounds reported in the manuscript was established through HPLC methodology. All the compounds reported in the manuscript have a purity > 95%.

General Synthetic Procedures. 3-(3,4-Dichlorophenyl)-1H-pyrrole-2,5-dione (62). To a stirred slurry of maleimide (**61**), anhydrous CuCl_2 and *tert*-butyl nitrite in CH_3CN at 0 °C a solution of 3,4-dichloro aniline in CH_3CN was added dropwise. The reaction mixture was stirred at room temperature for 1 h, and 20% aqueous HCl was added. The mixture was extracted with ethyl acetate, and the organic layer was washed with saturated aqueous NaCl and dried over Na_2SO_4 . To a solution of the crude obtained in 2-propanol, 2,6-lutidine was added and the mixture was warmed at reflux for 30 min. After elimination of the solvent under vacuum, the crude was dissolved in ethyl acetate and the organic phase washed with water and dried over sodium sulfate. The organic phase was concentrated under vacuum and the crude treated with diethyl ether. The solid was filtrated and dried under vacuum to give the title compound as brown solid. MS m/z 241 [M – H][–].

Ethyl-1-(3,4-dichlorophenyl)-2,4-dioxo-3-azabicyclo[3.1.0]hexane-6-carboxylate (63). Sodium hydroxide 60% in mineral oil was added in small portions to a stirred solution of (ethoxy-carbonylmethyl)-dimethylsulfonium bromide in anhydrous DMSO (20 mL). The resulting mixture was allowed to stir at room temperature for 1.5 h and then 3-(3,4-dichlorophenyl)-1H-pyrrole-2,5-dione (**62**) dissolved in DMSO (20 mL) was added dropwise, and the resulting mixture was stirred at room temperature for 1 min. Reaction temperature was brought to 0 °C, and aqueous saturated NH_4Cl was slowly added, followed by Et_2O . After separation of the two phases, the organic layer was washed twice with water and brine, and dried over Na_2SO_4 . Evaporation of the solvent under vacuum gave a crude compound which was purified by flash chromatography (eluting with ethyl acetate/cyclohexane 20:80) to give the title compound. MS m/z 326 [M – H][–].

[1-(3,4-Dichlorophenyl)-3-azabicyclo[3.1.0]hex-6-yl]methanol (2). To a stirred solution of **63** in of dry THF, BH_3 –THF complex in THF was slowly added at 0 °C under N_2 . The reaction mixture was refluxed for 6 h and then cooled to 0 °C, and aqueous HCl was added cautiously and the reaction mixture stirred for 1 h. The solvent was partially removed under vacuum, and the residue was loaded on mixed-mode strong cation exchange (MCX) column eluting with NH_3/MeOH (2M). The methanolic phase was evaporated under vacuum and the crude was purified by flash chromatography and separated through chiral HPLC to give the title compound. NMR (¹H, CDCl_3): δ 7.40 (m, 2H), 7.38 (d, 1H), 7.14 (dd, 1H), 3.51 (dd, 1H), 3.41 (dd, 1H), 3.32 (d, 1H), 3.12 (m, 2H), 2.91 (d, 1H), 1.69 (m, 1H), 1.39 (m, 1H). MS m/z 258 [MH]⁺.

1-(3,4-Dichlorophenyl)-6-[(methyloxy)methyl]-3-azabicyclo[3.1.0]hexane (4). To a stirred solution of **2** in dichloromethane at room temperature, triethylamine and bis(1,1-dimethylethyl)dicarbonate were added. Stirring was continued for 6 h, and

then the reaction mixture was concentrated under vacuum and the crude product treated with dichloromethane and bicarbonate. The organic phase was dried over sodium sulfate and the solvent evaporated under vacuum to give a crude product. To a stirred solution of this crude material in dry DMF, sodium hydride was added at 0 °C and the reaction mixture stirred at room temperature for 1 h. Methyl iodide was added, and the reaction mixture was stirred at room temperature for 4 h. Ethyl acetate and water were added and the organic phase separated, washed with brine, dried over sodium sulfate, and the solvent evaporated under vacuum to give a crude product. To a solution of this crude in DCM, TFA was added. The reaction mixture was stirred at room temperature for 1 h, it was concentrated in vacuo and the crude product was loaded on SCX column eluting with MeOH/NH_3 . The crude material obtained was purified by flash chromatography (eluting with dichloromethane/methanol/ammonia aq 95:5:0.5) to give 5 mg of the title compound as white oil. This was submitted to semipreparative HPLC to give the separated enantiomers by using a chiral column chiralpak AD-H, eluent A: *n*-hexane; B: ethanol, gradient isocratic 18% B, flow rate 14 mL/min, detection UV at 230 nm. Retention times given were obtained using an analytical HPLC using a chiral column chiralpak AD-H, 25 cm × 4.6 cm, eluent A: *n*-hexane; B: ethanol, gradient isocratic 20% B, flow rate 0.8 mL/min, detection UV at 230 nm. NMR (¹H, CDCl_3): δ 7.41 (d, 1H), 7.39 (d, 1H), 7.16 (dd, 1H), 3.30 (d, 1H), 3.21 (s, 3H), 3.20–3.10 (m, 4H), 3.90 (d, 1H), 1.74 (m, 1H), 1.37 (m, 1H). MS m/z 272 [MH]⁺. Retention time = 8.54 min.

Other compounds were prepared similarly. Further details can be found in refs 12 and 13.

6-[(Cyclopropylmethyl)oxy]methyl-1-(3,4-dichlorophenyl)-3-azabicyclo[3.1.0]hexane (9). NMR (¹H, DMSO): δ 9.86–8.13 (br s, 2H), 7.73–7.70 (d, 1H), 7.62–7.58 (d, 1H), 7.42–7.36 (dd, 1H), 3.81–3.70 (d, 1H), 3.52–3.45 (dd, 1H), 3.41–3.36 (d, 1H), 3.28–3.22 (dd, 1H), 3.20–3.14 (d, 1H), 3.09–3.02 (dd, 1H), 2.95–2.80 (m, 2H), 2.24–2.14 (m, 1H), 1.68–1.54 (m, 1H), 0.88–0.74 (m, 1H), 0.45–0.20 (m, 2H), –0.06–0.09 (m, 2H). Retention time = 7.54 min.

1-(3,4-Dichlorophenyl)-6-[(propyloxy)methyl]-3-azabicyclo[3.1.0]hexane (13). NMR (¹H, CDCl_3): δ 9.24 (br s 2H), 7.72 (d, 1H), 7.60 (d, 1H), 7.39 (dd, 1H), 3.78 (d, 1H), 3.50 (dd, 1H), 3.40 (d, 1H), 3.23 (m, 1H), 3.16 (m, 2H), 2.97 (m, 1H), 2.91 (dd, 1H), 2.22 (m, 1H), 1.66 (m, 1H), 1.34 (m, 2H), 0.73 (t, 3H). MS m/z 300 [MH]⁺. Retention time = 5.49 min.

1-(3,4-Dichlorophenyl)-6-[(ethyloxy)methyl]-3-azabicyclo[3.1.0]hexane (15). NMR (¹H, CDCl_3): δ 7.43 (s, 1H), 7.37 (d, 1H), 7.18 (d, 1H), 3.41–3.20 (m, 4H), 3.15 (s, 2H), 3.07 (m, 1H), 2.91 (d, 1H), 1.94 (m, 1H), 1.63 (m, 1H), 1.38 (m, 1H), 1.13 (t, 3H), NH not observed. MS m/z 286 [MH]⁺. Retention time = 7.0 min.

6-[(Ethyloxy)methyl]-3-methyl-3-azabicyclo[3.1.0]hexane (18). NMR (¹H, CDCl_3): δ 7.42 (s, 1H), 7.35 (d, 1H), 7.15 (d, 1H), 3.38–3.28 (m, 2H), 3.26–3.12 (m, 3H), 3.05–2.97 (m, 1H), 2.54 (m, 1H), 2.33 (s, 3H), 2.32 (m, 1H), 1.98 (m, 1H), 1.61 (m, 1H), 1.07 (t, 3H). MS m/z 300 [MH]⁺.

1-(3,4-Dichlorophenyl)-6-[[2,2,2-trifluoroethyl]oxy]methyl]-3-azabicyclo[3.1.0]hexane (20). NMR (¹H, CDCl_3): δ 7.41 (m, 2H), 7.16 (d, 1H), 3.67–3.51 (m, 3H), 3.35 (d, 1H), 3.27 (t, 1H), 3.16 (m, 2H), 2.92 (d, 1H), 1.67 (s, 1H), 1.41 (m, 1H). MS m/z 340 [MH]⁺. Retention time = 6.0 min.

1-(3,4-Dichlorophenyl)-6-[(1-methylethyl)oxy]methyl]-3-azabicyclo[3.1.0]hexane (23). NMR (¹H, CDCl_3): δ ppm 7.48 (1 H, d), 7.39 (1 H, d), 7.19 (1 H, dd), 3.36–3.46 (2 H, m), 3.24–3.35 (3 H, m), 2.94–3.06 (2 H, m), 1.65–1.71 (1 H, m), 1.44–1.53 (1 H, m), 1.08 (3 H, d), 1.01 (3 H, d). MS m/z 300 [MH]⁺. Retention time = 8.6 min.

6-[(Cyclobutyl)oxy]methyl-1-(3,4-dichlorophenyl)-3-azabicyclo[3.1.0]hexane Hydrochloride (25). NMR (¹H, CDCl_3): δ ppm 7.42–7.49 (m, $J = 1.26$ Hz, 1 H), 7.16 (dd, $J = 8.15, 1.45$ Hz, 1 H), 3.65–3.78 (m, 1 H), 3.33 (d, $J = 11.49$ Hz, 1 H), 3.13–3.23

(m, 3 H), 2.87–3.04 (m, 2 H), 1.97–2.20 (m, 4 H), 1.80–1.92 (m, 1 H), 1.58–1.72 (m, 3 H), 1.33–1.51 (m, 2 H). MS m/z 312 [MH]⁺. Retention time = 7.9 min.

6-[(Cyclohexyloxy)methyl]-1-(3,4-dichlorophenyl)-3-azabicyclo[3.1.0]hexane (28). NMR (¹H, CDCl₃): δ ppm 7.46 (d, 1 H), 7.37 (d, 1 H), 7.17 (dd, 1 H), 3.60–3.68 (m, 1 H), 3.30–3.39 (m, 2 H), 3.13–3.17 (m, 2 H), 2.87–2.97 (m, 2 H), 1.30–1.86 (m, 11 H). MS m/z 326 [MH]⁺. Retention time = 5.2 min.

6-[(Cyclohexyloxy)methyl]-1-(3,4-dichlorophenyl)-3-azabicyclo[3.1.0]hexane (30). NMR (¹H, CDCl₃): δ ppm 10.43 (br s, 1 H), 9.72 (br s, 1 H), 7.51 (d, 1 H), 7.44 (d, 1 H), 7.20 (dd, 1 H), 3.69–3.79 (m, 1 H), 3.54–3.69 (m, 2 H), 3.31–3.42 (m, 2 H), 2.95–3.09 (m, 2 H), 1.98 (t, 1 H), 1.57–1.86 (m, 5 H), 1.44–1.53 (m, 1 H), 1.11–1.23 (m, 5 H). MS m/z 340 [MH]⁺.

1-(3,4-Dichlorophenyl)-6-[(4-fluorophenyl)oxy]methyl]-3-azabicyclo[3.1.0]hexane (31). NMR (¹H, CDCl₃): δ ppm 7.43 (s, 1 H), 7.36 (d, 1 H), 7.18 (d, 1 H), 6.92 (m, 2 H), 6.70 (m, 2 H), 3.82 (m, 1 H), 3.60 (m, 1 H), 3.36 (d, 1 H), 3.19 (s, 2 H), 2.95 (d, 1 H), 2.15 (bs, 1 H), 1.75 (m, 1 H), 1.58 (m, 1 H). MS m/z 352 [MH]⁺.

1-(3,4-Dichlorophenyl)-3-azabicyclo[3.1.0]hex-6-yl]methyl]-dimethylamine (32). To a stirred solution of **2** in dichloromethane at room temperature, triethylamine and bis(1,1-dimethylethyl) dicarbonate were added. Stirring was continued for 6 h and then the reaction mixture was diluted with dichloromethane and quenched with a saturated solution of NH₄Cl. The organic phase was dried and the solvent evaporated under vacuum. Dess–Martin periodinane was added at 25 °C, and after 30 min, sodium thiosulfate and a saturated NaHCO₃ aqueous solution were added and the mixture was stirred at room temperature for 30 min. The mixture was then extracted with dichloromethane; the organic phase was washed with brine, dried over Na₂SO₄, and concentrated in vacuo. The compound was dissolved in dry tetrahydrofuran, and dimethylamine (0.349 mL), acetic acid (0.043 mL), and sodium triacetoxyborohydride (173 mg) were added at 25 °C. After 1 h stirring at room temperature, the mixture was concentrated in vacuo. Dichloromethane was then added, and the organic phase was washed with an aqueous saturated NaHCO₃ solution and brine, dried over Na₂SO₄, and concentrated in vacuo. The crude material was purified by flash chromatography (Biotage Si 12S column, gradient cyclohexane/ethyl acetate from 90/10 to 0/100 and then ethyl acetate/methanol 100/1) to give the title compound as a colorless oil. NMR (¹H, CDCl₃): δ ppm 7.40–7.32 (m, 2 H), 7.09 (m, 1 H), 3.30 (d, 1 H), 3.15 (s, 2H), 2.96 (d, 1 H), 2.40 (m, 1 H), 2.20 (s, 6 H), 2.19 (bs, 1 H), 1.75–1.62 (m, 2 H), 1.20 (m, 1 H). MS m/z 285 [MH]⁺.

1-(3,4-Dichlorophenyl)-6-[(methylthio)methyl]-3-azabicyclo[3.1.0]hexane (34). To a stirred solution of **2** in dichloromethane at room temperature, triethylamine and bis(1,1-dimethylethyl) dicarbonate were added. Stirring was continued for 6 h and then the reaction mixture was diluted with dichloromethane and quenched with a saturated solution of NH₄Cl. The organic phase was dried and the solvent evaporated under vacuum. The compound was dissolved in THF, and triethylamine and methanesulfonyl chloride were added at 0 °C. The reaction mixture was stirred at 25 °C for 1 h, and then water was added and the mixture was extracted with dichloromethane. The organic phase was washed with an aqueous saturated NH₄Cl solution, dried over Na₂SO₄, and concentrated in vacuo. It was dissolved in dry *N,N*-dimethylformamide, and sodium thiomethoxide was added. The mixture was stirred overnight at room temperature. An aqueous saturated NaHCO₃ solution was then added, and the mixture was extracted with dichloromethane. The organic phase was washed with brine, dried over Na₂SO₄, and concentrated in vacuo and dissolved in dry dichloromethane; trifluoroacetic acid was added at room temperature. After 30 min, the reaction mixture was concentrated in vacuo and the residue was purified by a SCX cartridge to give the title compound.

The enantiomers of the title compound were separated by chiral HPLC by using a chiral column Chiralcel OJ-H (25 cm × 0.46 cm), eluent A: *n*-hexane; B: 2-propanol + 0.1% isopropylamine, isocratic 4% B, 10% B from 27 min, flow rate 1 mL/min, detection UV at 210–340 nm, CD 230 nm. Retention times given were obtained using an analytical HPLC using a chiral column Chiralcel OJ-H (25 cm × 0.46 cm), eluent A: *n*-hexane; B: 2-propanol + 0.1% isopropylamine, isocratic 4% B, flow rate 1 mL/min, detection UV at 210–340 nm, CD 230 nm. NMR (¹H, CDCl₃): δ ppm 7.42–7.32 (m, 2 H), 7.11 (m, 1 H), 3.32 (d, 1 H), 3.17 (s, 2H), 2.95 (d, 1 H), 2.40 (m, 1 H), 2.20–2.10 (m, 1 H), 2.10 (s, 3 H), 2.06 (bs, 1 H), 1.68 (m, 1 H), 1.32 (m, 1 H). MS m/z 288 [MH]⁺. Retention time = 17.2 min.

1-(3,4-Dichlorophenyl)-6-propyl-3-azabicyclo[3.1.0]hexane (36). To a stirred solution of **2** in dichloromethane at room temperature, triethylamine and bis(1,1-dimethylethyl) dicarbonate were added. Stirring was continued for 6 h and then the reaction mixture was diluted with dichloromethane and quenched with a saturated solution of NH₄Cl. The organic phase was dried, and the solvent evaporated under vacuum. The compound was dissolved in THF, and triethylamine and methanesulfonyl chloride were added at 0 °C. The reaction mixture was stirred at 25 °C for 1 h, and then water was added and the mixture was extracted with dichloromethane. The organic phase was washed with an aqueous saturated NH₄Cl solution, dried over Na₂SO₄, and concentrated in vacuo. The compound was dissolved in THF and added to a stirred solution of copper(I) bromide–dimethylsulfide complex and EtMgBr 3 M in diethyl ether kept at –78 °C for 30 min. The mixture was heated to room temperature and stirred for 3 h. The reaction mixture was quenched saturated NH₄Cl aqueous solution and filtered off through celite. The filtrate was washed with an ammonia solution and extracted with ethyl acetate. The extract was dried over Na₂SO₄ and concentrated in vacuo. The residue dissolved in CH₂Cl₂, and TFA was added at 0 °C. The reaction was left for 2 h at rt, and it was concentrated in vacuo; the residue was purified by a SCX cartridge. NMR (¹H, CDCl₃): δ ppm 9.66 (bs, 1H), 7.45 (d, 1 H), 7.30 (d, 1H), 7.09 (m, 1 H), 3.70 (d, 1 H), 3.56 (m, 2H), 3.36 (bs, 1H), 1.8 (s, 1 H), 1.48 (s, 1 H), 1.38–1.28 (m, 3 H), 0.90–0.78 (m, 3 H). MS m/z 271 [MH]⁺. Retention time = 17.2 min.

6-[(Methyloxy)methyl]-1-(2-naphthalenyl)-3-azabicyclo[3.1.0]hexane (39). The racemate was separated by SFC HPLC using a chiral column Chiralcel OD-H, 25 cm × 0.46 cm, eluent ethanol + 0.1% isopropylamine 25%, flow rate 2 mL/min, detection UV at 230 nm. Retention time = 12.7 min. NMR (¹H, CDCl₃): δ ppm 7.86–7.76 (m, 4H), 7.52–7.45 (m, 3H), 3.44 (d, 1H), 3.28–3.25 (m, 3H), 3.19 (s, 3H), 3.15–3.04 (m, 2H), 1.84 (m, 1H), 1.45 (m, 1H).

1-(3,4-Dichlorophenyl)-3-azabicyclo[3.1.0]hex-6-yl]ethanol (40). To a stirred solution of **2** in dichloromethane at room temperature, triethylamine and bis(1,1-dimethylethyl) dicarbonate were added. Stirring was continued for 6 h and then the reaction mixture was diluted with dichloromethane and quenched with a saturated solution of NH₄Cl. The organic phase was dried and the solvent evaporated under vacuum. Dess–Martin periodinane was added at 25 °C, and after 30 min, sodium thiosulfate and a saturated NaHCO₃ aqueous solution were added and the mixture was stirred at room temperature for 30 min. The mixture was then extracted with dichloromethane; the organic phase was washed with brine, dried over Na₂SO₄, and concentrated in vacuo to give the crude **64**. To a stirred suspension of methyl(triphenyl)phosphonium bromide in THF at 0 °C, butyllithium (2.5 M in hexane) was added dropwise. The dark-yellow reaction mixture was allowed to reach room temperature and stirred for 20 min and then cooled to 0 °C, and the above-described crude **64** in THF was added dropwise. The ice-bath was removed and the reaction mixture stirred for 6 h at room temperature. Diethyl ether and water were added, the organic phase was dried on sodium sulfate, the solvent

evaporated *under vacuum*, and the crude product was purified by flash chromatography to achieve intermediate **65**. The intermediate was dissolved in THF at 0 °C, and under a nitrogen atmosphere, BH₃-THF complex (1 M in THF) was added dropwise. The ice-bath was removed and the reaction mixture stirred for 3.5 h at room temperature. The mixture was cooled to 0 °C and quenched by adding water. Then 3 M NaOH and 30% H₂O₂ were added and the resulting mixture stirred for 0.5 h. The reaction mixture was diluted with water and extracted with ethyl acetate; the organic phase was dried over Na₂SO₄ and the solvent removed under reduced pressure. The compound was dissolved in CH₂Cl₂, and TFA was added at room temperature. After 1 h, the reaction mixture was evaporated under vacuum, the residue dissolved in methanol, and 1 M NaOH was added. After 0.5 h, the solvent was removed under vacuum and the residue dissolved in CH₂Cl₂. The organic phase was separated through a separator phase cartridge and the solvent evaporated under reduced pressure to give the title compound.

NMR (¹H, CDCl₃): δ ppm 7.38 (d, 1 H) 7.32–7.34 (m, 1 H) 7.08 (dd, 1 H) 3.59–3.63 (m, 2 H) 3.31 (d, 1 H) 3.10–3.13 (m, 2 H) 2.93 (d, 1 H) 1.68 (none, 18 H) 1.50–1.61 (m, 2 H) 1.08–1.30 (m, 3 H). MS *m/z* 272 [MH]⁺.

1-(3,4-Dichlorophenyl)-6-[2-(methyloxy)ethyl]-3-azabicyclo[3.1.0]hexane (42). To a stirred solution of **40** in THF, at room temperature, NaH (60% in oil) was added portion wise. After 20 min, methyl iodide was added dropwise and the resulting reaction mixture was stirred overnight. Diethyl ether and aqueous saturated NH₄Cl were added, the organic phase washed with brine, dried on Na₂SO₄, and evaporated under reduced pressure to give the crude N-Boc intermediated. This product was dissolved in CH₂Cl₂, TFA was added, and the reaction mixture was stirred at room temperature for 1 h. After this period of time, the mixture was evaporated under reduced pressure and the residue dissolved in CH₂Cl₂, washed with 1 M NaOH, and separated through a phase separator cartridge. The organic phase was evaporated under reduced pressure to give the title compound as an oil which was submitted to semipreparative chiral chromatography (column: Chiralcel OD-H (25 cm × 0.46 cm), mobile phase: *n*-hexane/2-propanol 95/5% v/v; flow rate: 1.0 mL/min; DAD: 210–340 nm; CD: 230 nm). NMR (¹H, CDCl₃): δ ppm 7.37 (dd, 1 H) 7.31–7.34 (m, 1 H) 7.07 (dd, 1 H) 3.25–3.36 (m, 6 H) 3.06–3.12 (m, 2 H) 2.91 (d, 1 H) 1.49–1.59 (m, 2 H) 1.23–1.30 (m, 2 H). MS *m/z* 286 [MH]⁺. Retention time = 18.8 min.

1-(3,4-Dichlorophenyl)-6-[2-(ethyloxy)ethyl]-3-azabicyclo[3.1.0]hexane (44). Prepared in analogy to **42**. NMR (¹H, CDCl₃): δ ppm 7.37 (d, 1 H) 7.32 (d, 1 H) 7.04–7.10 (m, 1 H) 3.39–3.47 (m, 2 H) 3.28–3.39 (m, 3 H) 3.10–3.15 (m, 2 H) 2.93 (d, 1 H) 1.55–1.60 (m, 2 H) 1.15–1.21 (m, 4 H) 0.89–0.94 (m, 1 H). MS *m/z* 300 [MH]⁺.

1-(3,4-Dichlorophenyl)-6-[(5-methyl-1,3-oxazol-2-yl)methyl]-3-azabicyclo[3.1.0]hexane (45). To a stirred solution of **2** in dichloromethane at room temperature, triethylamine and bis(1,1-dimethylethyl) dicarbonate were added. Stirring was continued for 6 h, and then the reaction mixture was diluted with dichloromethane and quenched with a saturated solution of NH₄Cl. The organic phase was dried and the solvent evaporated under vacuum. The compound was dissolved in acetone, and at 0 °C, Jones reagent was added dropwise. After quenching and recovery of the product, the compound was dissolved in CH₂Cl₂; 1-hydroxybenzotriazole monohydrate and *N*-(3-dimethylaminopropyl)-*N'*-ethylcarbodiimide hydrochloride were added. Subsequently, propargyl amine was added dropwise and the reaction mixture was stirred at rt overnight. After quenching and work up, the crude product was dissolved in glacial acetic acid, mercury(II) acetate was added, and the reaction mixture was heated to 110 °C and stirred for 2.5 h. The solvent was removed under vacuum and the residue dissolved in ethyl acetate. The organic phase was washed with saturated NaHCO₃ and then brine and dried over sodium

sulfate. The solvent was evaporated under reduced pressure to give a crude product, which was purified by flash chromatography. This compound was dissolved in CH₂Cl₂, TFA was added, and the reaction mixture was stirred at rt for 1 h. The reaction mixture was concentrated under reduced pressure and the residue was partitioned between DCM and saturated aqueous NaHCO₃. The mixture was passed through a phase separator cartridge and the organic phase evaporated to give crude title compound. NMR (¹H, CDCl₃): δ ppm 7.30–7.40 (m, 2 H) 7.05–7.10 (m, 1 H) 6.58–6.61 (m, 1 H) 2.91–3.45 (m, 4 H) 2.40–2.61 (m, 2 H) 2.20–2.30 (m, 3 H) 1.72–1.79 (m, 1 H) 1.48–1.59 (m, 1 H). MS *m/z* 323.05 [MH]⁺.

1-(3,4-Dichlorophenyl)-6-(4-methyl-1,3-thiazol-2-yl)-3-azabicyclo[3.1.0]hexane (46). To a stirred solution of **2** in dichloromethane at room temperature, triethylamine and bis(1,1-dimethylethyl) dicarbonate were added. Stirring was continued for 6 h and then the reaction mixture was diluted with dichloromethane and quenched with a saturated solution of NH₄Cl. The organic phase was dried and the solvent evaporated under vacuum. The compound was dissolved in acetone, and at 0 °C, Jones reagent was added dropwise. After quenching and work up, the compound was dissolved in AcOEt and *N,N'*-carbonyldiimidazole was added. The mixture was stirred for 1.5 h at rt. The mixture was then cooled to 0 °C, and concentrated NH₄OH was added. After quenching and recovery of the compound, Lawesson's reagent was used to prepare the corresponding thioamide, which was subsequently dissolved in toluene and chloroacetone was added. The reaction mixture was heated at 80 °C for 3 h. On cooling to room temperature, the solvent was removed under vacuum and the residue taken up in CH₂Cl₂. TFA was added, and the reaction mixture was stirred for 2 h at rt. The reaction mixture was concentrated under reduced pressure, the residue dissolved in CH₂Cl₂, and purified using a SCX cartridge. NMR (¹H, CDCl₃): δ ppm 7.19–7.36 (m, 2 H) 7.01 (dd, 1 H) 6.47–6.61 (m, 1 H) 3.05–3.54 (m, 4 H) 2.67–2.73 (m, 1 H) 2.47–2.54 (m, 1 H) 2.30–2.34 (m, 3 H). MS *m/z* 325 [MH]⁺.

1-(3,4-Dichlorophenyl)-6-[(4-methyl-1,3-thiazol-2-yl)methyl]-3-azabicyclo[3.1.0]hexane (47). Derivative N-BOC protected derivative **40** was dissolved in acetone, and Jones reagent was added dropwise 0 °C. After quenching and work up, the compound was dissolved in EtOAc and *N,N'*-carbonyldiimidazole followed by concentrated NH₄OH at 0 °C. To a stirred solution of the crude amide in THF at rt, Lawesson's reagent was added portion wise. The mixture was heated to 80 °C and stirred for 3 h. The intermediate thioamide obtained was reacted with toluene, and the mixture was stirred for 3 h at 80 °C. The solution was concentrated under reduced pressure to give a residue. This product was dissolved in CH₂Cl₂, TFA was added, and the reaction mixture was stirred at rt for 1 h. The reaction mixture was concentrated under reduced pressure and purified to give the title product. NMR (¹H, CDCl₃): δ ppm 7.31–7.41 (m, 2 H) 7.05–7.12 (m, 1 H) 6.70–6.74 (m, 1 H) 3.30–3.40 (m, 1 H) 3.12–3.19 (m, 2 H) 2.86–3.01 (m, 2 H) 2.56–2.66 (m, 1 H) 2.36–2.44 (m, 3 H) 1.74–1.79 (m, 1 H) 1.47–1.54 (m, 1 H). MS *m/z* 339 [MH]⁺.

6-(3,4-Dichlorophenyl)-6-[(ethyloxy)methyl]-3-azabicyclo[3.1.0]hexane (60). To a solution of methyl diazo(3,4-dichlorophenyl)acetate in toluene, maleimide was added and the reaction mixture was refluxed for 4 h. The solvent was removed under reduced pressure, and the residue was purified via flash chromatography. To a solution of the compound thus obtained in dry THF, at 0 °C, BH₃·THF complex 1 M in THF was added and then the reaction mixture was refluxed for 4 h. MeOH and HCl 1 M in Et₂O were added, and the solution was stirred at rt overnight. The mixture was concentrated in vacuo, and the residue was purified by SCX cartridge. To a solution of this intermediate in CH₂Cl₂ at 0 °C, di-*tert*-butyl dicarbonate was added and the reaction mixture was stirred at rt overnight. After quenching and work up, the crude was purified by flash chromatography (Si 25M) to afford two isomers. The *exo* (NMR

(^1H , CDCl_3): δ ppm: 7.48 (s, 1H), 7.41 (d, 1H), 7.23 (d, 1H), 3.91–3.84 (m, 2H), 3.75–3.60 (m, 4H), 2.03 (s, 2H), 1.49 (s, 9H), 1.32 (t, 1H)) one was in dry CH_2Cl_2 and at 0 °C, TEA (40 μL) and methanesulfonylchloride (28.6 μL) were added and the reaction mixture was stirred at rt overnight. After quenching and work up, the compound was dissolved in dry DMF and EtONa in dry DMF was added at 0 °C. The reaction mixture was stirred at rt for 3 h and then 1 h at 60 °C. Aqueous NH_4Cl saturated solution was added and then extracted with Et_2O . The combined organic phases were washed with aqueous NaCl saturated solution, dried, and concentrated in vacuo. To a solution of the compound in CH_2Cl_2 , at 0 °C, TFA was added and then the reaction mixture was stirred at rt for 2 h. The solution was concentrated in vacuo, and the residue was purified by SCX cartridge to give the title compound. NMR (^1H , CDCl_3): δ ppm 7.39 (d, 1 H) 7.31 (d, 1 H) 7.14 (dd, 1 H) 3.78 (s, 2 H) 3.41–3.42 (m, 2 H) 3.27–3.33 (m, 2 H) 3.21–3.26 (m, 2 H) 1.87–1.94 (m, 2 H) 1.13 (t, 3 H). MS m/z 286 $[\text{MH}]^+$.

6-(3,4-Dichlorophenyl)-3-azabicyclo[3.1.0]hexane (52). NMR (^1H , MeOD) δ ppm 7.59 (s, 1 H) 7.47 (d, 1 H) 7.31 (d, 1 H) 3.74–3.81 (m, 4 H) 3.49 (d, 2 H) 3.40–3.28 (m, 2 H) 2.42 (s, 2 H) 1.02 (t, 1 H) 0.52–0.50 (m, 2 H) 0.19–0.18 (m, 2 H). MS m/z 312 $[\text{MH}]^+$.

6-[(Cyclobutyl)oxy]methyl]-6-(3,4-dichlorophenyl)-3-azabicyclo[3.1.0]hexane (53). NMR (^1H , MeOD) δ ppm 7.52–7.59 (m, 1 H) 7.48 (d, 1 H) 7.30 (dd, 1 H) 3.86–4.00 (m, 1 H) 3.78 (d, 2 H) 3.61 (s, 2 H) 3.37–3.49 (m, 2 H) 2.41 (s, 2 H) 0.78–2.25 (m, 6 H). MS m/z 312 $[\text{MH}]^+$.

6-(3,4-Dichlorophenyl)-6-[(2,2,2-trifluoroethyl)oxy]methyl]-3-azabicyclo[3.1.0]hexane (54). NMR (^1H , DMSO- d_6) δ ppm 9.70 (bs, 1 H) 9.43 (bs, 1 H) 7.58 (m, 2 H) 7.29 (d, 1 H) 4.09 (q, 2 H) 3.94 (s, 2 H) 3.64 (m, 2 H) 3.31 (m, 2 H) 2.39 (s, 2 H). MS m/z 340 $[\text{MH}]^+$.

6-(3,4-Dichlorophenyl)-6-[(1-methylpropyl)oxy]methyl]-3-azabicyclo[3.1.0]hexane (55). NMR (^1H , CDCl_3) δ ppm 7.46 (s, 1 H) 7.36 (d, 1 H) 7.18 (d, 1 H) 3.72–3.87 (dd, 2 H) 3.22–3.36 (m, 5 H) 1.95 (s, 2 H) 1.35–1.60 (m, 2 H) 1.09 (d, 3 H) 0.85 (t, 3 H).

6-(3,4-Dichlorophenyl)-6-[2-(methoxy)ethyl]-3-azabicyclo[3.1.0]hexane Hydrochloride (56). To a solution of methyl diazo-(3,4-dichlorophenyl)acetate in toluene, maleimide was added and the reaction mixture was refluxed for 4 h. The solvent was removed under reduced pressure, and the residue was purified via flash chromatography. To a solution of the compound thus obtained in dry THF, at 0 °C, $\text{BH}_3 \cdot \text{THF}$ complex 1 M in THF was added and then the reaction mixture was refluxed for 4 h. MeOH and HCl 1 M in Et_2O were added and the solution was stirred at rt overnight. The mixture was concentrated in vacuo, and the residue was purified by SCX cartridge. To a solution of this intermediate in CH_2Cl_2 at 0 °C, di-*tert*-butyl dicarbonate was added and the reaction mixture was stirred at rt overnight. After quenching and work up, the crude was purified by flash chromatography (Si 25M) to afford two isomers. The exo isomer in dry CH_2Cl_2 at 0 °C, was added with Dess–Martin periodinane portion wise, and then the reaction mixture was stirred at rt overnight. The compound thus obtained was dissolved in and added dropwise to a stirred solution of the preformed ylide obtained by addition of BuLi to methyltriphenylphosphonium bromide in dry THF at 0 °C. After quenching and work up, the compound was dissolved in dry THF at 0 °C, and borane THF complex 1 M in THF was added dropwise. The ice-bath was removed, and the reaction mixture was stirred for 3.5 h at rt. The solution was then quenched at 0 °C with water, and NaOH 3 M and H_2O_2 were added; the resulting mixture was stirred at 0 °C for 0.5 h. After quenching and work up, the compound was dissolved in DMF, NaH was added at 0 °C, and the reaction mixture was stirred at rt for 30 min. Iodomethane was added to the reaction mixture, and then the temperature was increased to 40 °C. After quenching and work up, the crude was purified to give the title compound. NMR (^1H , MeOD) δ ppm 7.40–7.60 (m, 2 H) 7.27 (dd, 1 H) 3.72 (d, 2 H) 3.42–3.57 (m,

2 H) 3.24–3.30 (m, 5 H) 2.24–2.36 (m, 2 H) 1.86 (t, 2 H). MS m/z 286 $[\text{MH}]^+$.

6-(3,4-Dichlorophenyl)-6-[2-(ethoxy)ethyl]-3-azabicyclo[3.1.0]hexane (57). NMR (^1H , CDCl_3) δ ppm 10.35 (s, 1 H) 9.72 (s, 1 H) 7.33–7.44 (m, 2 H) 7.07–7.15 (m, 1 H) 3.70–3.84 (m, 2 H) 3.64 (d, 2 H) 3.40 (q, 2 H) 3.29 (t, 2 H) 2.17 (s, 2 H) 1.89 (t, 2 H) 1.08–1.27 (m, 3 H). MS m/z 300 $[\text{MH}]^+$.

6-(3,4-Dichlorophenyl)-6-[2-[(1-methylethyl)oxy]ethyl]-3-azabicyclo[3.1.0]hexane (58). NMR (^1H , DMSO- d_6) δ ppm 9.47–9.79 (m, 1 H) 8.81–9.08 (m, 1 H) 7.50–7.67 (m, 2 H) 7.16–7.37 (m, 1 H) 3.52–3.65 (m, 2 H) 3.36–3.47 (m, 1 H) 3.23–3.32 (m, 2 H) 3.13–3.23 (m, 2 H) 2.15–2.27 (m, 2 H) 1.73–1.85 (m, 2 H) 1.03 (d, 6 H). MS m/z 314 $[\text{MH}]^+$.

Acknowledgment. We thank all the colleagues who helped in generating the data reported in this manuscript, in particular Dr. A. Feriani and Dr. D. Dal Ben. We also thank Dr. D. Donati, Dr. J. Hagan, and Dr. T. Rossi for their support during the programme life.

Supporting Information Available: An example of TRUI minimal pharmacophore construction. This material is available free of charge via the Internet at <http://pubs.acs.org>.

References

- (1) (a) Kulkarni, S. K.; Dhir, A. Current investigational drugs for major depression. *Exp. Opin. Investig. Drugs* **2009**, *18*, 767–788. (b) Wong, M. L.; Licinio, J. From monoamines to genomic targets: a paradigm shift for drug discovery in depression. *Nat. Rev. Drug Discovery* **2004**, *3*, 136–151. (c) Millan, M. J. The role of monoamines in the actions of established and “novel” antidepressant agents: a critical review. *Eur. J. Pharmacol.* **2004**, *500*, 371–384. (d) Nemeroff, C. B. The burden of severe depression: a review of diagnostic challenges and treatment alternatives. *J. Psychiatry Res.* **2007**, *41*, 189–206.
- (2) (a) Arnt, J.; Christensen, A. V.; Hyttel, J. Pharmacology in vivo of the phenylindan derivative, Lu-19,005, a new potent inhibitor of dopamine, noradrenaline, and 5-hydroxytryptamine uptake in rat brain. *Arch. Pharmacol.* **1985**, *329*, 101–107. (b) Chen, Z.; Skolnick, P. Triple uptake inhibitors: therapeutic potential in depression and beyond. *Expert Opin. Investig. Drugs* **2007**, *16*, 1365–1377. (c) Rakofsky, J. J.; Holtzheimer, P. E.; Nemeroff, C. B. Emerging targets for antidepressant therapies. *Curr. Opin. Chem. Biol.* **2009**, *13*, 291–302. (d) Liang, Y.; Shaw, A. M.; Boules, M.; Briody, S.; Robinson, J.; Oliveros, A.; Blazar, E.; Williams, K.; Zhang, Y.; Carlier, P. R.; et al. Antidepressant like pharmacological profile of a novel triple reuptake inhibitor, (1S,2S)-3-(methylamino)-2-(naphthalen-2-yl)-1-phenylpropan-1-ol (PRC200-SS). *J. Pharmacol. Exp. Ther.* **2008**, *327*, 573–583. (e) Skolnick, P.; Popik, P.; Janowsky, A.; Beer, B.; Lippa, A. S. “Broad spectrum” antidepressants: is more better for the treatment of depression? *Life Sci.* **2003**, *73*, 3175–3179. (f) Aluisio, L.; Lord, B.; Barbier, A. J.; Fraser, I. C.; Wilson, S. J.; Boggs, J.; Dvorak, L. K.; Letavic, M. A.; Maryanoff, B. E.; Carruthers, N. I. In vitro and in vivo characterization of JNJ-7925476, a novel triple monoamine uptake inhibitor. *Eur. J. Pharmacol.* **2008**, *587*, 141–146. (g) Bannwart, L. M.; Carter, D. S.; Cai, H. Y.; Choy, J. C.; Greenhouse, R.; Jaime-Figueroa, S.; Iyer, P. S.; Lin, C. J.; Lee, E. K.; Lucas, M. C. Novel 3,3-disubstituted pyrrolidines as selective triple serotonin/norepinephrine/dopamine reuptake inhibitors. *Bioorg. Med. Chem. Lett.* **2008**, *18*, 6062–6066. (h) Papakostas, G. I. Dopaminergic-based pharmacotherapies for depression. *Eur. Neuropsychopharmacol.* **2006**, *16*, 391–402. (i) Skolnick, P.; Popik, P.; Janowsky, A.; Beer, B.; Lippa, A. S. Antidepressant-like actions of DOV21,947: a “triple” reuptake inhibitor. *Eur. J. Pharmacol.* **2003**, *461*, 99–104.
- (3) (a) Scheel-Kruger, J.; Moldt, P.; Watjen, F. Tropane-derivatives, their preparation and use. U.S. Patent 6395748, **2002**; (b) Scheel-Kruger, J.; Moldt, P.; Watjen, F. Tropane-derivatives, their preparation and use. U.S. Patent 6288079, **2001**; (c) Scheel-Kruger, J.; Moldt, P.; Watjen, F. Tropane-derivatives, their preparation and use. Patent WO 9730997, **1997**; (d) Scheel-Kruger, J.; Olsen, G. M.; Nielsen, E. O.; Dahl, B. H.; Jensen, L. H. Fused tropane derivatives as neurotransmitter reuptake inhibitors. Patent WO 9716451, **1997**.
- (4) (a) *Maestro*, version 8.5.111; Schrodinger LLC: New York, **2006**; (b) *BatchMin*, version 9.6; Schrodinger LLC: New York, **2006**; (c) *Phase*, version 3.0.110; Schrodinger LLC: New York, **2006**.

- (5) The research complied with national legislation and with company policy on the Care and Use of Animals and with related codes of practice.
- (6) Minick, D. J.; Rutkowske, R. D.; Miller, L. A. D. Strategies for successfully applying vibrational circular dichroism in a pharmaceutical research environment. *Am. Pharmaceut. Rev.* **2007**, *10*, 118–123.
- (7) Aptuit Limited, 3 Simpson Parkway, Livingston, West Lothian, EH54 7BH, Scotland; www.apuit.uk.
- (8) Zocchi, A.; Fabbri, D.; Heidbreder, C. A. Aripiprazole increases dopamine but not noradrenaline and serotonin levels in the mouse prefrontal cortex. *Neurosci. Lett.* **2005**, *387*, 157–161.
- (9) Burchall, C. J.; Soroko, F. E.; Rigdon, G. C. Potentiation of the behavioral effects of 5-hydroxytryptophan by BW 1370U87, a selective monoamine oxidase-A inhibitor. *Drug Dev. Res.* **1992**, *25*, 209–213.
- (10) Martin, G. E.; Bendesky, R. J. Mouse locomotor activity: an in vivo test for dopamine autoreceptor activation. *J. Pharmacol. Exp. Ther.* **1984**, *229*, 706–711.
- (11) Bourin, M.; Chenu, F.; Prica, C.; Hascoet, M. Augmentation effect of combination therapy of aripiprazole and antidepressants on forced swimming test in mice. *Psychopharmacology (Heidelberg, Ger.)* **2009**, *206*, 97–107.
- (12) Bonanomi, G.; Micheli, F.; Terreni, S. Azabicyclic compounds as serotonin, dopamine and norepinephrine re-uptake inhibitors and their preparation, pharmaceutical compositions and use in the treatment of depression. Patent WO 2008074716, **2008**.
- (13) Bertani, B.; Bonanomi, G.; Di Fabio, R.; Fazzolari, E.; Micheli, F.; Tarsi, L. Preparation of 3-azabicyclo[3.1.0]hexane compounds as monoamine neurotransmitter re-uptake inhibitors. Patent WO 2009027293, **2009**.